Static Structural Analysis of Fighter Aircraft's Wing Spars

Usama Tariq, Farrukh Mazhar
College of Aeronautical Engineering National
University of Science and Technology
usama15029009@gmail.com
farrukhmazhar@cae.nust.edu.pk

***Abstract*— This study aims at describing a methodology for the Static Structural Analysis of Fighter Aircraft's wing spars for identification of critical stresses. Aircraft's wing is subjected to various flight loads i.e. bending loads, twisting loads, shear stress etc. This analysis helps to determine structural and material safety limit of aircraft's wing. Also, the location of critical stresses, that arises due to different loading actions on both wing and wing spars, can be determine. The failure of aircraft wing while performing different maneuvers like pulling g's can cause catastrophic results. Therefore, for safety concerns, different analysis was done on aircraft's wing. So, in this paper, bending stress, shear stress and von mises stress was calculated analytically and numerically for different loading conditions and then critical stresses were formulated and identified for failure or yielding points of wing spars. For ANSYS Simulation, CAD Models of wing and wing spars were imported in ANSYS workbench and static structural analysis was done to obtain critical stresses. Von Mises yield theory was used to formulate and identify critical stresses and yielding stresses. Numerical stress simulation was done in ANSYS and results for Von Mises Stress were obtained for different loading conditions. The results obtained from using both analytical calculation and numerical simulation were analyzed. Some of the ANSYS simulated results were exceeding beyond yield limit at some loading conditions and these exceeding results for both wing and spars were marked as critical stresses. The locations of these critical stresses were at attachment or fixed point of wing spars.**

***Keywords*—-Static Structural Analysis, Wing Spars, Critical Stresses, Von Mises's Stress, Factor of Safety**

I. INTRODUCTION

Wing and fuselage are the two major components of aircraft. Wing has primary ability to carry the bending loads. Wings are attached at right angle to the fuselage and are fixed from one side so they act like a cantilever beam. Wing is subjected to different types to loads mainly containing loads due to lift, fuel, engine, landing gear, inertial, structural, and other aerodynamic effect. Spars are the main structural members with ability to bear these loads. Spars are beams or structural members which are running along the wing and they carry different forces and moments due to distribution of lift along the span of wing.

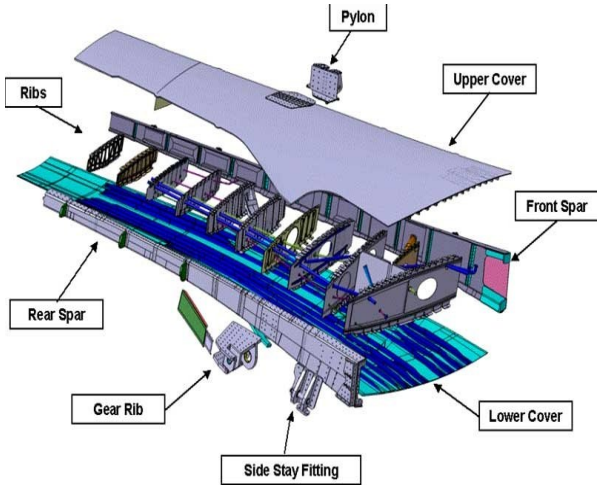

Fig. 70: Aircraft Wing [1]

Since Aircraft wing is subjected to various repeated loading during flying so it must have high value of strength to weight ratio to withstand these loads. Static structural analysis is used to calculate values of deformations and stresses acting on wing

978-0-7381-0535-2/21/$31.00 ©2021 IEEE

due to these repeated loads. These loads are acting at different g's values and wing must be constructed strong enough to counter these loads. Wing must be made using high strength materials.

LITERATURE REVIEW

1. Aircraft Wing

To fly an aircraft, the aircraft must be able to lift the load or weight of itself, fuel, pilot, passengers and cargo. The maximum amount of lift is generated by wings to help the aircraft fly. The engines provide the required thrust to help the aircraft fly through the air. Small wings are present at horizontal and vertical tails to help in control and provide maneuverability to the aircraft. The tail usually contains a horizontal stabilizer (fixed horizontal part) and a vertical stabilizer (fixed vertical part). These stabilizers help to provide stability and control the maneuverability of aircraft.

The spars are the most supportive part of wing running along the wing in spanwise direction at right angle to fuselage. The wings weight and loads acting during flying are carried by spars so they must be made of strong material to hold the twisting and bending loads or else it will cause failure of wing and eventually catastrophic results. Ribs are also attached with spars to help in carry almost all types of loads along with spars like bending, torsion, tensile and compression. While the aircraft is on the ground spars and ribs help in carrying wings weight. Main spar carries major amount of total load acting on the wing. Usually a fighter aircraft has 3 spars.

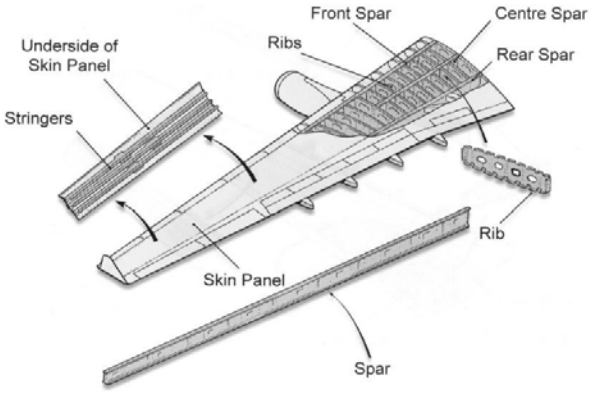

Fig. 71: Basic Structure of aircraft wing [2]

2. Wing Spars

A wing has spars and ribs to carry different loads acting on the wing. Spars are running spanwise while ribs are located chordwise in the wing. The spars can be considered as cantilever beam. Due to different loads acting on the wing, shear stress and pressure is generated on wing along the chord and spars and ribs carries these reactions and hold the wing strong to bear them.Ribs help in keeping the airfoil shape of the wing as they are present along the chord of wing and also help in resisting the torsion and twisting effect of the wing. Stringers are present in the wing to help in carrying surface loads of wing to spars and ribs and they also help in resisting the bending of wing due to various application of loads on the wing. Spars can be made of different materials like wood, composites and metals. It depends on specific design criteria of aircraft. According to cross-sectional configuration spars can be classified into four different types as I beam, box shaped, solid and partly hollow [3].

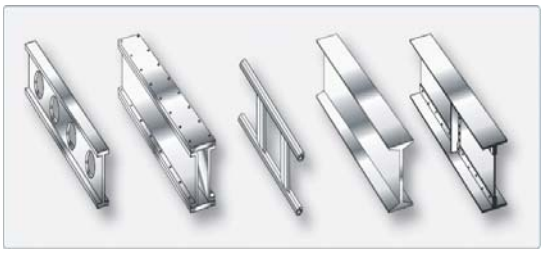

Fig.72: Configurations of Spar Beam [4]

For analysis, I-beam spar configuration is used for analytical calculation of main spar.

3. I-Beam Spars

Caps are the top and bottom part of the I–beam and web is the center vertical section. One metal can be used to make the entire spar but it is often made up more than one angle or extrusions. The main principal depth is formed by web and caps are attached to the web. Together, caps and webs carry he bending loads of wing and wing skin is attached to the caps portion [4].

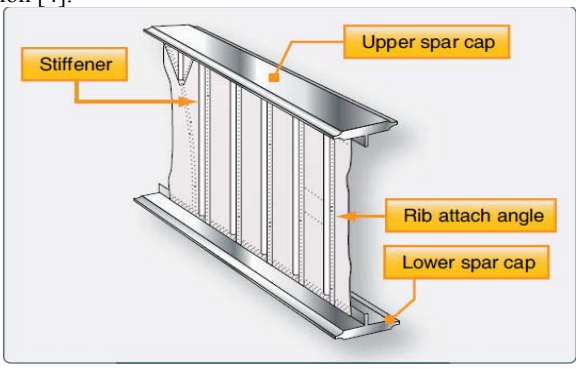

Fig.73: I-Beam Spar [4]

4. Spar loads

Spars are the most important part of wing as they are responsible to support maximum load acting on the wing. While the combination of spars and ribs provide rigidity and strength to wing which makes aircraft fly safely. In Biplanes flying wires are employed to transmit loads during flight through the wires which enables small and light weighted spars to be used [3].

5. Forces acting on spar

Following are the forces acting on wing spars [3]

- bending loads acting upward and downward due to lift force and wings weight respectively.
- Drag loads that are induced due to airspeed and due to effect of inertia.
- Inertial loads due to rolling.
- Twisting loads that are acting chordwise while flying at high airspeed and these loads are due to aerodynamic effects.

6. ANSYS

Ansys is an analyzing software and is used to simulate computer build models of structures, machine components or electronics to obtain strength, fluid flow, elasticity, toughness and other attributes. It can determine different functions of computer build model under different conditions without making actual test model. These models are meshed into smaller parts to carryout different operations. CAD model is imported into Ansys and then different conditions are applied like pressure, force, moment, temperature or other physical properties and then Ansys will simulate under applied conditions to determine required results like deformations, fatigue, factor of safety, Stresses, strains, fluid flow etc. [10].

7. LoadFactor

During flying, a stress is produced on aircraft due to applied force that deflects the aircraft from straight line flight, this force is called as load factor. Load factor is defined as ratio of aerodynamic force to total weight of aircraft. For example, load factor of 4 means that amount of load acting on aircraft is 4 times its weight [5].

$$\textbf{Load Factor} = \frac{\textbf{Lift}}{\textbf{Weight}} \quad (1)$$

When an aircraft is design, it is necessary to determine maximum load factor which can be expected in different operational conditions. These maximum load factors are called limit load factors. For safety concerns, an aircraft should be designed in a way to withstand various highest load factors without having any structural damage. During level flight, wings provide support to weight of the aircraft and also to centrifugal force experienced by aircraft. As an aircraft takes steep bank, load factor increases due to increase in horizontal component of lift and centrifugal force. But if the value of load factor increases so much that increase in angle of attack don't provide enough amount of lift to support the load, the wing stalls. Since stall speed increases directly with square root of load factor, pilot have to be aware of different flight conditions due to which load factor can increase to a critical value. If we increase g's value, weight of aircraft and load acting on wing will also increase by respective increase in g's values. During flying an aircraft interacts with air and in result, drag force acts on the aircraft[5].

$$Drag\ Force = 0.5 \times p \times K^2 \times S \times C_d \quad (2)$$

$$Lift\ Force = 0.5 \times p \times K^2 \times S \times C_l \quad (3)$$

The below fig. shows the schematic diagram [52] of high g maneuvers performed by aircraft while it is performing pitch and turning maneuvers.

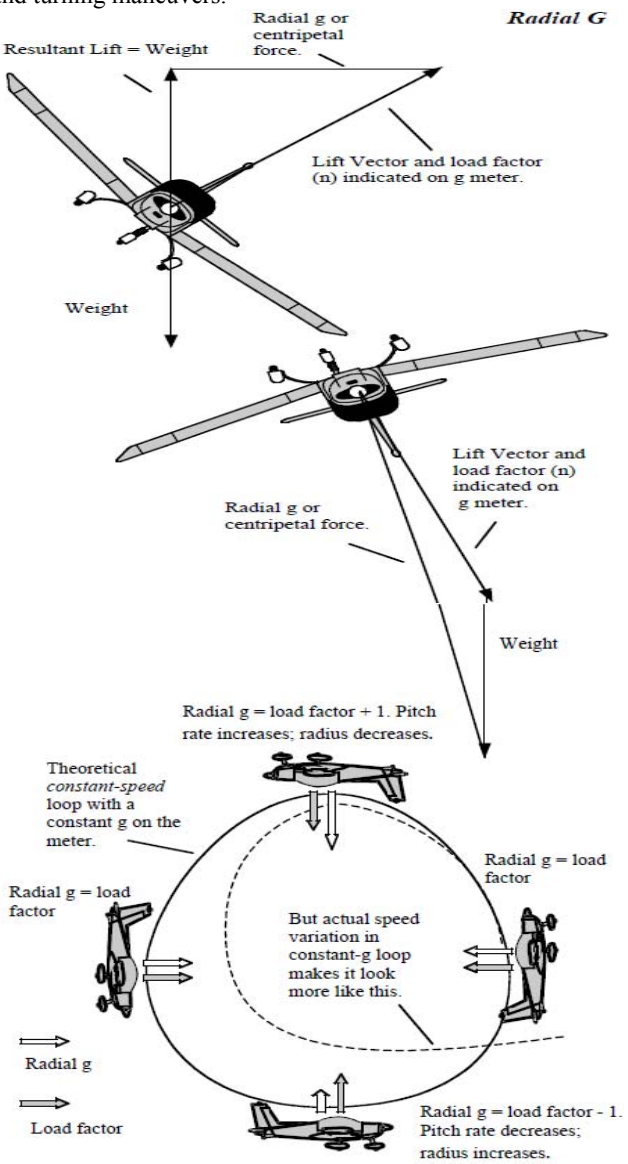

8. Von Mises's Theory

There are many theories to discuss the failure of material, Von Mises theory is used to predict the yielding of material. This theory states that a material (ductile) will yield/fail when the distortion energy per volume reaches a critical value. The critical value of the distortional energy can be used to estimate [8]. State of stresses at yielding point is given by:

$\sigma_1=\sigma_Y$ (yield stress)

$\sigma_2=\sigma_3 = 0$

At yielding distortion energy per volume is:

$$U_d = \frac{1+v}{3E} {S_Y}^2 \quad (4)$$

$$U_d = \frac{1+v}{3E} {\sigma_{VM}}^2 \geq U_d = \frac{1+v}{3E} {S_Y}^2 \quad (5)$$

$$\boldsymbol{{\sigma_{VM}}^2 \geq {S_Y}^2} \quad (6)$$

Where,
σ_Y= Yield Stress
U_d = Distortion Energy per Volume
v = Poisson Ratio
E = Elastic Modulus
σ_{VM} = Von Mises's Stress
S_Y = Yield Strength

Thus, the theory of distortion energy states that in uniaxial tensile test material yields as the value of von Mises stress becomes greater than the yielding stress [8].

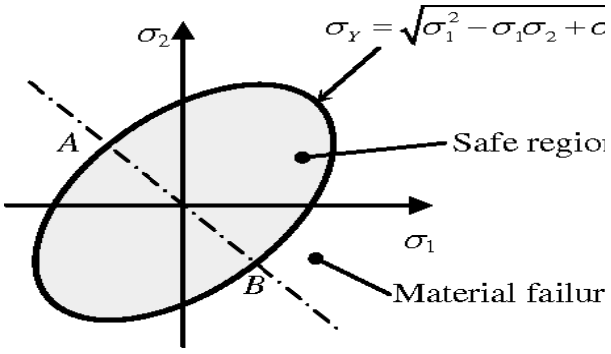

Fig. 74: Failure Envelope of Distortion Energy Theory to find yielding of material in tensile test [9]

Maximum Distortion Energy Theory (Von Mises Yield Criterion):

Von Mises Stress for 3-D case

$$\sigma_0 = \sqrt{(\sigma_1 - \sigma_2)^2 + (\sigma_2 - \sigma_3)^2 + (\sigma_3 - \sigma_1)^2}$$

Von Mises Stress for 2-D case

$$\sigma_0 = \sqrt{({\sigma_1}^2 - \sigma_1\sigma_2 + {\sigma_2}^2)}$$

Yield Stress, σ_y, occurs when

$$\sigma_0 \geq \sigma_y$$

9. Factor of Safety

The ratio of the yield strength of a material to the maximum equivalent or von mises's stress is defined as factor of safety. In aerospace industry, 1.5 is the minimum factor of safety [8]. The origin of 1.5 factor of safety for aircraft both military and commercial was first established in 1934 and has been in use since that time.

$$\textbf{Factor of Safety} = \frac{\textbf{Yield Strength}}{\textbf{Von Mises Stress}}$$

10. Lift Distribution on Wing

A. Elliptical Lift distribution

To determine the loads acting on the wing, we must know about the lift distributed along the span of wing. There is elliptical distribution of lift in most aerodynamically efficient wing along the wingspan, with maximum value of lift at center and zero lift value at tip of wing. Most practical wing geometries have a spanwise lift distribution approaching elliptical, but with relatively small variations in spanwise lift distribution due to wing planform. Wing twist, flap deployment and changes in airfoil section along the wing will affect the distribution of lift along the span, and these effects should be taken into account where appropriate.

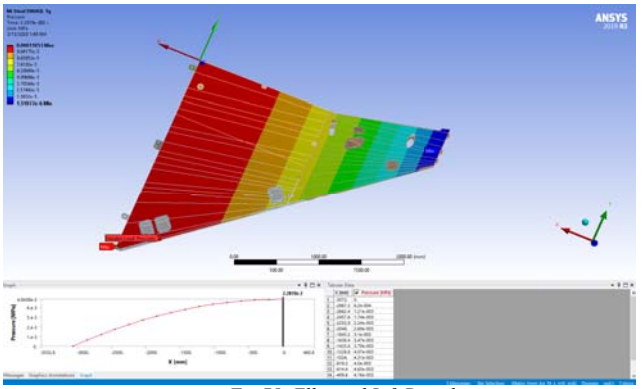

Fig.75: Elliptical Lift Distribution

$$\boldsymbol{w = w_0[1 - \frac{x^2}{L^2}]}$$

The upper equation is used to calculate elliptical pressure distribution. Then, the calculated pressure distribution is applied on lower side of wing and spar models in ANSYS using tabular data. It is done in Boundary condition section of Finite Element Analysis chapter.

For Analytical calculations and CATIA models simulations of spars in ANSYS, uniform pressure distribution is used.

B. Schrenk Approximation

This is a method to find solution for span-wise lift distribution. Schrenk method is the mean of planform lift and elliptical lift distributions.

$$L'_{\text{Elliptical}} = \frac{4L}{\pi b}\sqrt{1-(\frac{2y}{b})^2}$$

$$L'_{\text{Planform}} = \frac{2L}{(1+\lambda)b}(1+\frac{2y}{b}(\lambda-1))$$

$$L'_{\text{Schrenk}} = \frac{L'_{\text{Elliptical}} + L'_{\text{Planform}}}{2}$$

Where,

L: total lift force (N)
L': lift distribution (N/m)
λ: taper ratio
b: wing span (m)
y: spanwise distance of section (m)

II. METHODOLOGY AND RESULTS

For Static Structural Analysis of Fighter Aircraft's Wing Spars, we will be adopting the following methodology.

1. CAD model of Wing

We get the already available CAD model of the aircraft. Model mainly contain these major elements of wing internal structure that are as below.

- Spars
- Skin
- Ribs
- Wing attachment points tofuselage

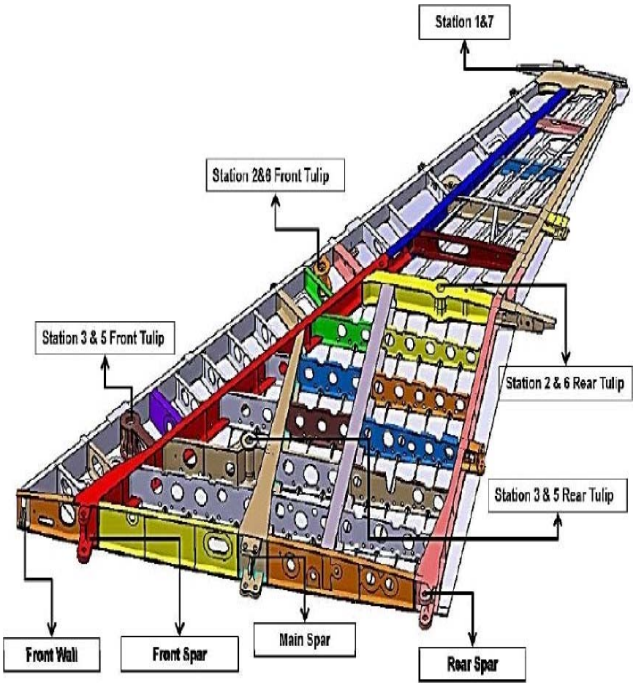

2. Assigned Materials to different Sections of wing

As a whole wing is major part of the aircraft but it has the different types of geometrieshavingdifferenttypeofmaterialsproperties.Dependin guontheposition of the part of wing the different mechanical properties were given as the standard aircraft pattern. For example, the all the spars of the wings take all the load that is acting on the wing so they are prefer to have a greater strength as compared to ribs and skin of thewing.

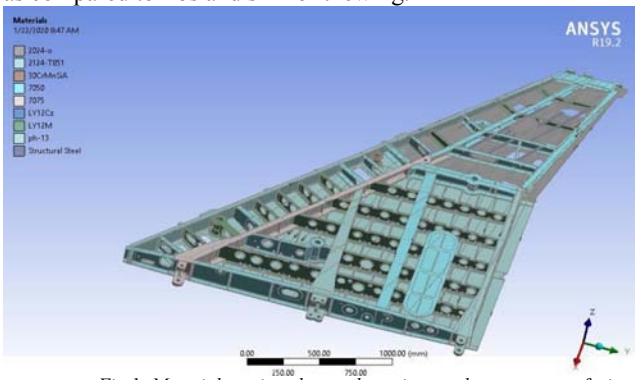

Fig.1: Materials assigned to each sections and components of wing

Each material along with its properties and areas where they are used in wing model in ANSYS are shown below,

A. AL-7075-T6 / AISI-7050

Table 1: Material properties of AL-7075-T6 / AISI-7050 [44]

Properties	Values
Ultimate Tensile Strength	572 MPa
Yield Strength	510 MPa
Poisson Ratio	0.33
Modulus of Elasticity	71.3 GPa

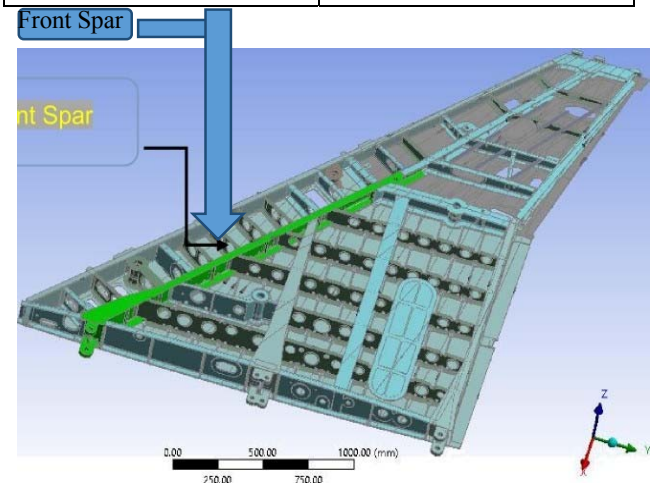

Fig.2: Materials assigned to section and component of wing

Fig.4: AISI S13800 Materials assigned to section and component of wing

B. AL-7050-T7451

Table 2: Material properties of AL-7075-T7451 [44]

Properties	Values
Ultimate Tensile Strength	524 MPa
Yield Strength	460 MPa
Poisson Ratio	0.33
Modulus of Elasticity	71.3 GPa

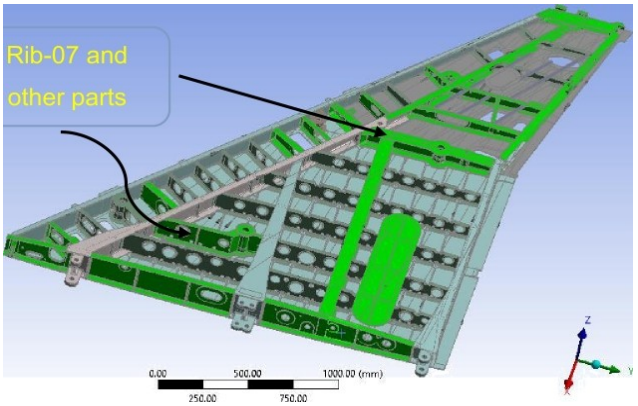

Fig.3: AL-7075-T7451 Material assigned to different sectionof the wing

C. PH 13-8 / AISI S13800

Table 3: Material properties of PH 13-8 / AISI S13800 [44]

Properties	Values
Ultimate Tensile Strength	1480 MPa
Yield Strength	1410 MPa
Poisson Ratio	0.22
Modulus of Elasticity	221 GPa

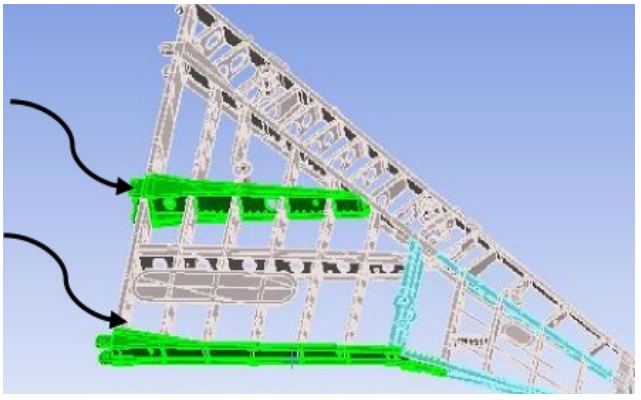

D. 2124-T851 / ASTM B209

Table 4: Material properties of* 2124-T851 / ASTM B209*[44]

Properties	Values
Ultimate Tensile Strength	483 MPa
Yield Strength	441 MPa
Poisson Ratio	0.33
Modulus of Elasticity	73.1 GPa

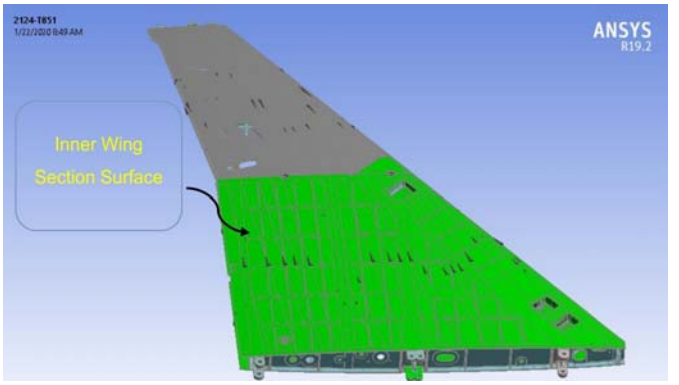

*Fig.5:*2124-T851 / ASTM B209 *Materials assigned to section and component of wing*

E. 30CrMnSiA / AISI 1024 Steel

***Table 5: Material properties of* 30CrMnSiA / AISI 1024 Steel [45]**

Properties	Values
Ultimate Tensile Strength	1080 MPa
Yield Strength	835 MPa
Poisson Ratio	0.3
Modulus of Elasticity	207 GPa

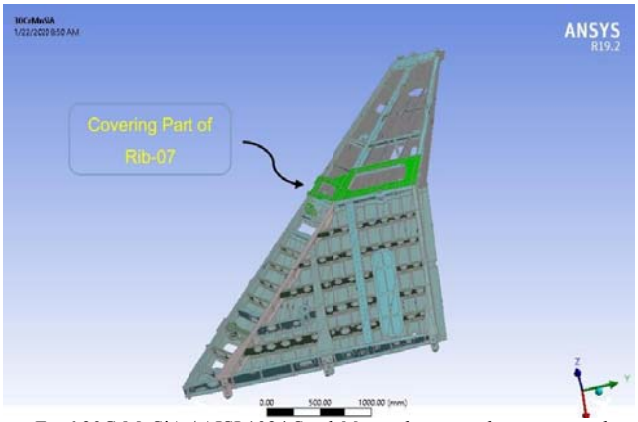

*Fig.6:*30CrMnSiA / AISI 1024 Steel *Materials assigned to section and component of wing*

F. LY 12m

***Table 6: Material properties of* LY 12m [46]**

Properties	Values
Ultimate Tensile Strength	186 MPa
Yield Strength	75.8 MPa
Poisson Ratio	0.33
Modulus of Elasticity	73.1 GPa

Fig.7: LY 12mMaterials assigned to section and component of wing

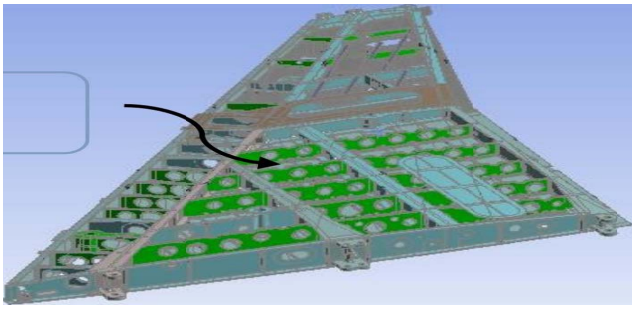

G. A l - 2024

***Table 7: Material properties of* AL-2024 [44]**

Properties	Values
Ultimate Tensile Strength	186 MPa
Yield Strength	75.8 MPa
Poisson Ratio	0.33
Modulus of Elasticity	73.1 GPa

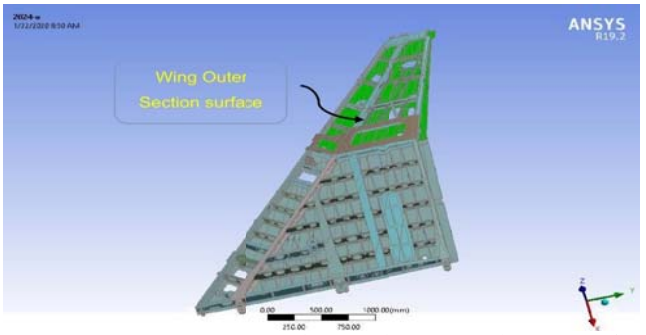

Fig.8: AL 2024Materials assigned to section and component of wing

H. LY12-Cz

***Table 8: Material properties of* LY12-cz [46]**

Properties	Values
Ultimate Tensile Strength	464 MPa
Yield Strength	320 MPa
Poisson Ratio	0.35
Modulus of Elasticity	70 GPa

Below materials are used in spars for analysis in ANSYS.

I. Structural Steel

***Table 9: Material properties of* Structural Steel [47]**

Properties	Values
Ultimate Tensile Strength	1150 MPa
Yield Strength	960 MPa
Poisson Ratio	0.3
Modulus of Elasticity	200 GPa

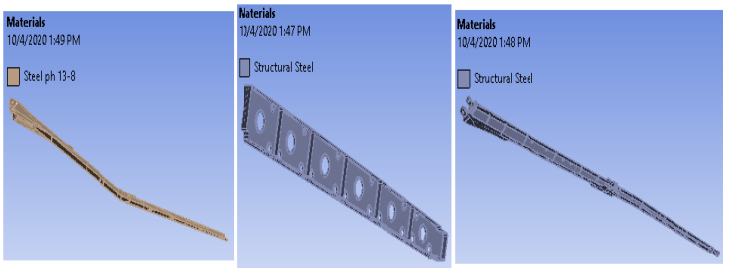

J. Titanium Ti-6Al-2Zr-2Sn-2Mo-2Cr-0.25Si (AMS 4898, Ti-6-22-22)

This titanium alloy is used in wing box of US F-22 Aircraft [49].

***Table 10: Material properties of* Titanium Ti-6Al-2Zr-2Sn-2Mo-2Cr-0.25Si**

Properties	Values

Ultimate Tensile Strength	1120 MPa
Yield Strength	1010 MPa
Poisson Ratio	0.33
Modulus of Elasticity	108 GPa

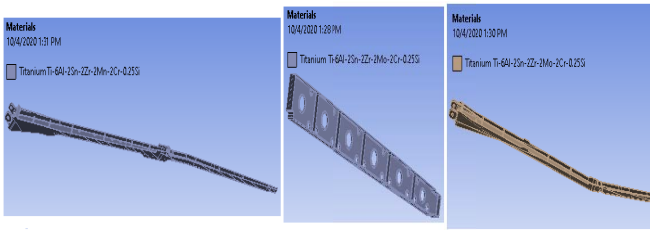

K. Titanium Ti-6Al-4V (ASTM Grade 5, Ti64, TC4)

This alloy is used wing spar cap strips of C919 aircraft using Laser Metal Deposition (LMD) technique in Northwestern Polytechnical University, China [50].

***Table 11: Material properties of* Titanium Ti-6Al-4V [48]**

Properties	Values
Ultimate Tensile Strength	950 MPa
Yield Strength	880 MPa
Poisson Ratio	0.342
Modulus of Elasticity	113.8 GPa

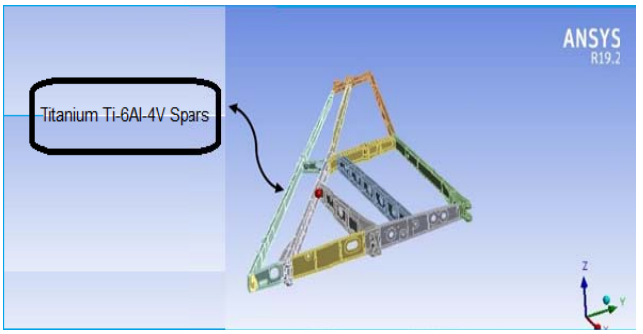

3. Finite Element Analysis Procedure:

Finite Element Analysis is performed on CAD model of wing and spars in ANSYS to obtain critical Von Mises stresses and factor of safety. The results are obtained for loading conditions and these results are compared with analytical results. This whole analysis is described step wise below.

4. Analytical Calculation

Load factor that we have for the flights have correspond the total number of cycles that are acting on the aircraft in form of vertical load factor Nz. This load factor can be converted into the loads that can be used in the finite element analysis. If we know about the load factor, we can calculate the value of lift produced by the aircraft at that time. For this calculation we take the maximum gross takeoff weight of the aircraft as we don't know about the actual weight of aircraft for that time. For more conservative approach it is going to good for us forusing Gross Take Off Weight (GTOW). Weightbasicallyistheproductofaccelerationandmassoftheobject atthattime.For the value of 1 g calculations are beingdone. For analytical calculations, only 2D state of stress is solved for calculation of stresses.
Gross Takeoff Weight of aircraft = m= 12,474 kg
Weight = W = mg = $12474 \times 9.81 = 122{,}369.94$ N

For Cruise condition,
Lift = Weight
Force = F = 122,369.94 N
It is assumed that 95% of the total lift is produced by wings
F = $0.95 \times 122{,}369.94 = 116{,}251.44$ N

The above value is the load acting on both wings. For single wing the load value will be,
F = $\frac{116{,}251.44}{2}$ = 58,125.72 N

Wing reference area = 24 m^2
For single wing, S_{ref}= 12 m^2

$$\text{Pressure} = \frac{F}{S_{ref}} = \frac{58{,}125.72}{12} = 4843.81 \text{ Pa}$$

The below table shows values of pressure at different g values. However, standard Earth gravity i.e. 9.81 $^{m}/_{s^2}$ is applied for all g's conditions.

Table 12: Pressure values

Load factor	Pressure value (MPa)
1g	0.00484381
2g	0.00968762
3g	0.01453143
4g	0.01937524
5g	0.02421905
6g	0.02906286
7g	0.03390667
8g	0.03875048

A. Main Spar

It is assumed that main spar is carrying 40% of applied load

F = $0.40 \times 58{,}125.72 = 23250.29$ N

Reference area of both wings is,
S_{ref}= 24 m^2

For single wing,
S_{ref}= 12 m^2

Pressure = $\frac{Force}{S_{ref}} = \frac{23250.29}{12}$ = 1937.52 Pa

Moment produced will be,
M = $Force \times Length$ = 23250.29 × 0.651 = 15135.94 Nm

The total length of I beam is 0.188m.
Centroid location will be,
$\bar{y}$ = 0.094 m

Since the wing is under flexural loading so bending stress and shear stress will be acting on the wing and their values are,
For cantilever beams, bending stress is given by,
$\sigma_{Bending} = \frac{M\bar{y}}{I}$

In above equation, only second moment of inertia (I) is unknown, So
Second Moment of Inertia = I = $\frac{bH^3}{12} + 2(\frac{Bh^3}{12} + \frac{hB(h+H)^2}{4})$
I = $1.345 \times 10^{-5} m^4$
$\sigma_{Bending} = \frac{M\bar{y}}{I} = \frac{15135.94 \times 0.094}{1.345 \times 10^{-5}}$ = 105.78 MPa

And shear stress is given by,
$\tau = \frac{VQ}{I_c t_w}$

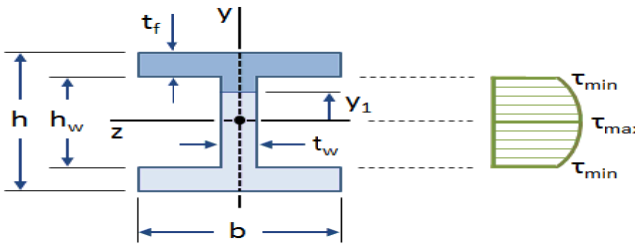

Where,
V = 23250.29 N
I = $1.345 \times 10^{-5} m^4$
t_w = 0.055 m
Q = $\frac{b}{8}(h^2 - {h_w}^2) + \frac{{t_w}^2}{8}({h_w}^2 - 4{y_1}^2)$

Q = $7.17 \times 10^{-5} m^3$
$\tau = \frac{VQ}{I_c t_w} = \frac{23250.29 \times 7.17 \times 10^{-5}}{1.345 \times 10^{-5} \times 0.055}$ = 2.25 MPa

Von Mises's Stress will be,
$\acute{\sigma} = \sqrt{{\sigma_{Bending}}^2 + 3\tau^2}$ = 105.85 MPa

This value of Von Mises stress exists near fixed end of cantilever I beam.
The solution obtained for von mises stress is for 2-D state of stress.

Factor of Safety:
Factor of safety for both materials will be,
Yield Strength of Structural Steel = 960 MPa
Yield Strength of Titanium = 1700 MPa
When the material is steel, FOS = $\frac{960}{105.85}$ = 9.59

When the material is titanium, FOS = $\frac{1700}{105.85}$ = 16.06

The above factor of safety is obtained when the wing is loaded under 1g condition. For different load factor and force values the Von Mises's Stress and Factor of safety will be,

Table 13: Analytical Results of main spar

G's Values	Force (MPa)	Von Mises's Stress (MPa)	Factor of Safety (Steel)	Factor of Safety (Titanium)
-1 g	23250.29	100.98	9.51	16.84
-2 g	46500.58	211.17	4.55	8.05
-3 g	69750.87	318.67	3.01	5.33
1 g	23250.29	105.85	9.59	9.59
2 g	46500.58	211.7	4.53	8.03
3 g	69750.87	317.57	3.02	5.34
4 g	93001.15	423.42	2.27	4.01
5 g	116251.44	490.29	1.96	3.47
6 g	139501.73	530.13	1.81	3.21
7 g	162752.02	567.60	1.69	2.99

While the results obtained using CAD model of I beam of main spar and simulating in ANSYS are,

Dimensions of I beam are,
Depth = 0.188 m
Width = 0.17 m
Flange Thickness = 0.004 m
Web Thickness = 0.055 m

The Catia model of I beam is shown below

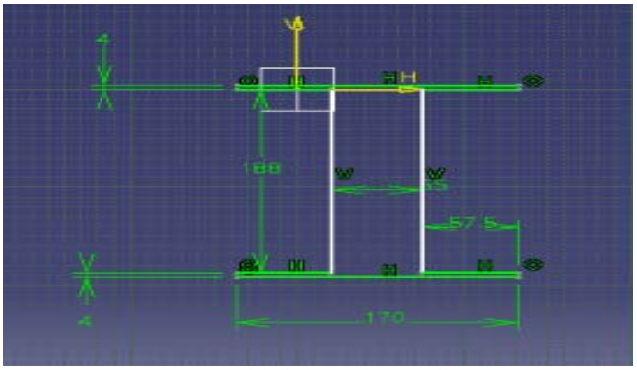

Fig. 9: CATIA Model of I beam Showing all Dimensions

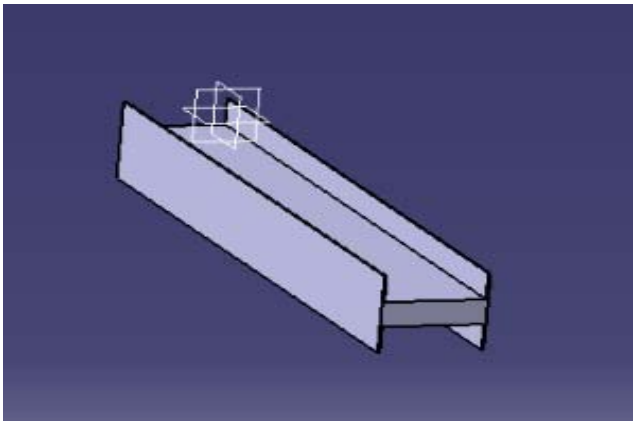

Fig. 10: 3-D CATIA Model of I Beam

This model of I beam is imported into ANSYS and static structural analysis is done to obtain Von Mises's Stress and Factor of Safety under different loading conditions with different g's values.

Steel and titanium are used as materials for I beam structure. Meshing is done to obtain required results. Boundary conditions applied are similar to that used for wing model previously i.e. Fixed from one side and upward force and downward gravitational acceleration is applied on I beam. In figure below A point shows fixed end, B shows gravity acting downward and C shows load acting on lower side of wing in upward direction. Fig. 12 and 13 shows von mises stress and factor of safety at 1g.

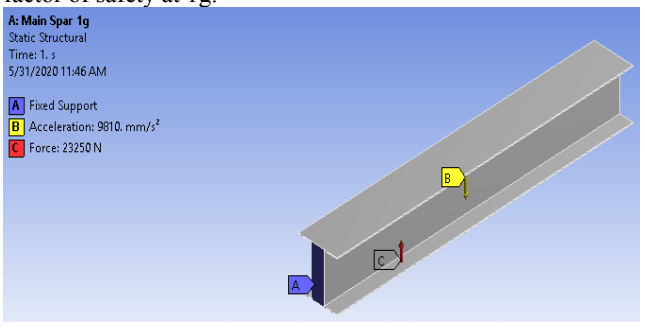

Fig. 11: Boundary Conditions applied at 1g condition

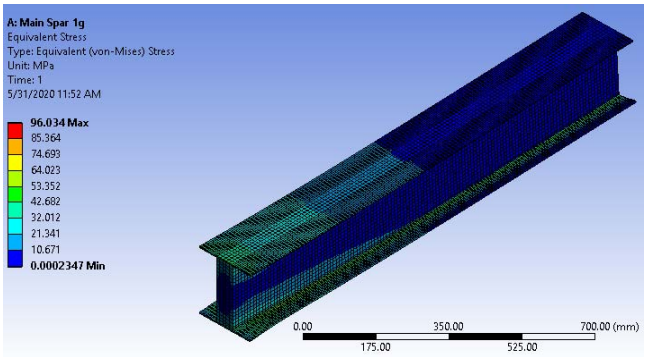

Fig. 12: Von Mises's Stress at 1g condition

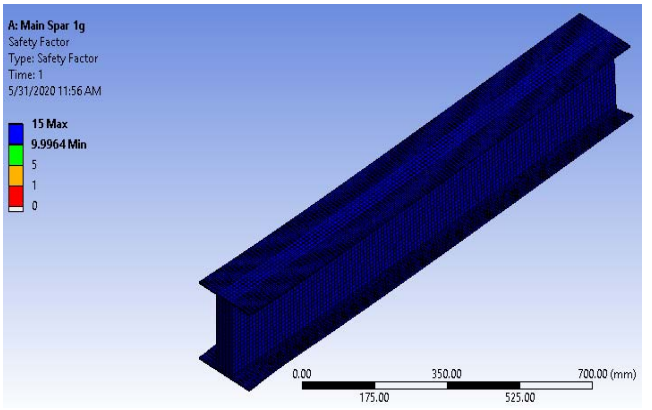

Fig. 13: Factor of Safety at 1g condition

Table 14: ANSYS Results for Main Spar using Steel

G's Values	Von Mises's Stress (MPa)	Factor of Safety
-1 g	90.07	10.65
-2 g	180.03	5.33
-3 g	270.04	3.55
-4 g	360.06	2.66
1 g	96.03	9.99
2 g	192.07	4.99
3 g	288.1	3.33
4 g	384.14	2.49
5 g	480.17	1.99
6 g	576.21	1.66

Table 15: ANSYS Results for Main Spar using Titanium

G's Values	Von Mises's Stress (MPa)	Factor of Safety
-1 g	90.54	18.77
-2 g	181.01	9.39
-3 g	271.52	6.26
-4 g	362.02	4.69
1 g	94.05	18.07
2 g	188.12	9.03
3 g	282.17	6.02
4 g	376.23	4.51
5 g	470.29	3.61
6 g	564.35	3.01
7 g	658.4	2.58
8 g	752.46	2.25

Error in FOS for Steel $= \frac{1.81-1.66}{1.81} \times 100 = 8.29\%$

Error in FOS for Titanium $= \frac{2.99-2.58}{2.99} \times 100 = 13.71\%$

B. Rear Spar

It is assumed rear spar is carrying 30% of total load acting on the wing.

Table 16: Analytical Results of Rear spar

G's Values	Force (MPa)	Von Mises's Stress (MPa)	Factor of Safety (Steel)	Factor of Safety (Titanium)
-1 g	17437.72	894.233	1.95	1.90
-2 g	34875.43	2178.55	0.80	0.78

-3 g	52313.15	3268.95	0.535	0.52
1 g	17437.72	894	1.95	1.90
2 g	34875.43	2179	0.80	0.8
3 g	52313.15	3269	0.54	0.52

Dimensions of C beam are,
Depth = 0.13 m
Width = 0.04 m
Flange Thickness = 0.004 m
Web Thickness = 0.004 m

The CATIA Model of C-Beam is shown below

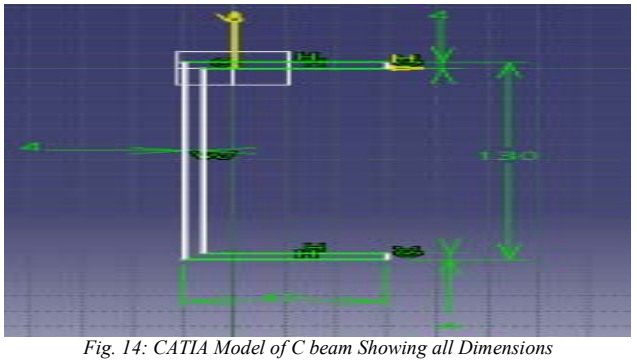

Fig. 14: CATIA Model of C beam Showing all Dimensions

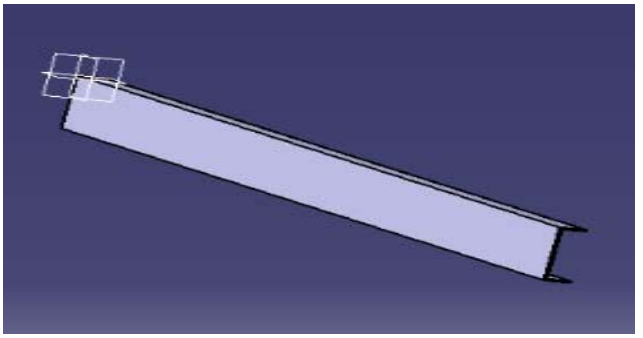

Fig. 15: 3-D CATIA Model of C Beam

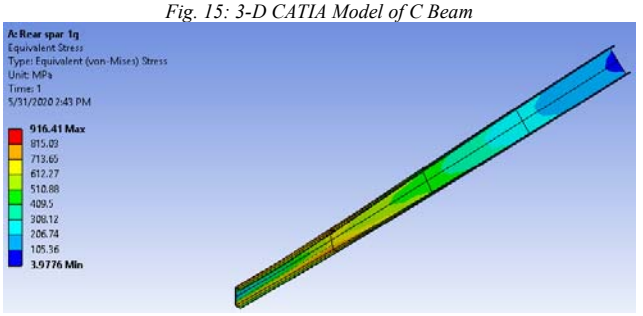

Fig. 16: Von Mises's Stress at 1g condition

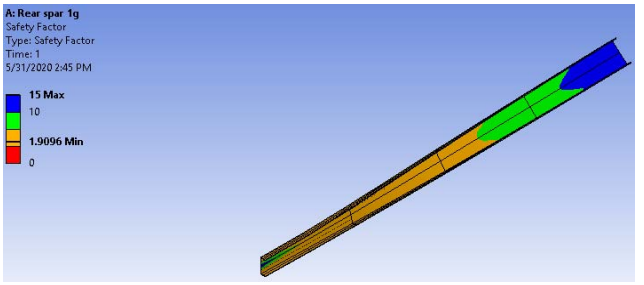

Fig. 17: Factor of Safety at 1g condition

Table 17: ANSYS Results for Rear Spar using Steel

G's Values	Von Mises's Stress (MPa)	Factor of Safety
-1 g	900.91	1.94
-2 g	1801.8	0.97
-3 g	2702.7	0.65
1 g	916.41	1.91
2 g	1832.8	0.95
3 g	2749.2	0.64

Table 18: ANSYS Results for Rear Spar using Titanium

G's Values	Von Mises's Stress (MPa)	Factor of Safety
-1 g	898.02	1.89
-2 g	1796	0.95
-3 g	2694	0.63
1 g	906.73	1.87
2 g	1813.5	0.94
3 g	2720.2	0.62

Error in FOS for Steel = $\frac{0.64-0.52}{0.64} \times 100 = 18.75\%$

Error in FOS for Titanium = $\frac{0.62-0.52}{0.62} \times 100 = 16.13\%$

C. Front Spar

It is assumed that front spar carries 30% of total load acting on the wing [59].

Table 19: Analytical Results of front spar

G's Values	Force (MPa)	Von Mises's Stress (MPa)	Factor of Safety (Steel)	Factor of Safety (Titanium)
-1 g	17437.72	50	10.03	34
-2 g	34875.43	100	5.02	17
-3 g	52313.15	150	3.34	11.33
1 g	17437.72	49.86	10.03	34.09
2 g	34875.43	99.72	5.01	17.04
3 g	52313.15	149.58	3.34	11.36
4 g	69750.87	199.46	2.51	8.52
5 g	87188.58	249.32	2.0	6.82
6 g	104626.30	299.18	1.67	5.68
7 g	122064.01	330.05	1.51	5.15

Dimensions of C beam are,
Depth = 0.185 m
Width = 0.175 m
Flange Thickness = 0.025 m
Web Thickness = 0.025 m
The CATIA Model of C-Beam is shown below

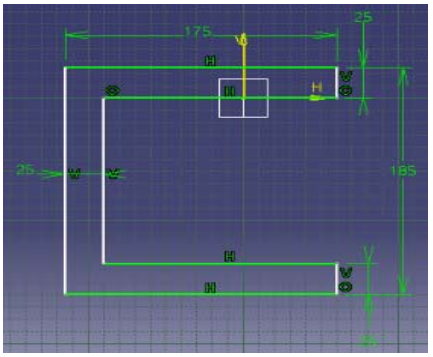

Fig. 18: CATIA Model of C beam Showing all Dimensions

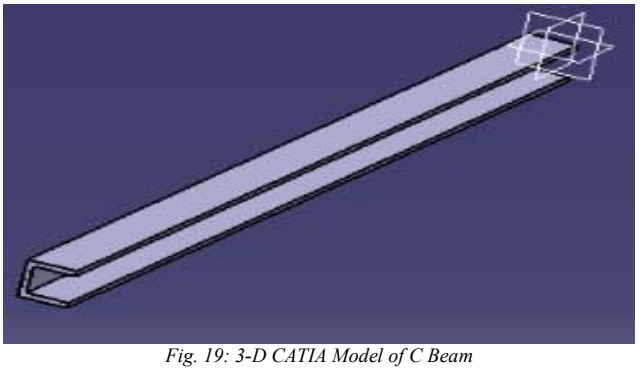

Fig. 19: 3-D CATIA Model of C Beam

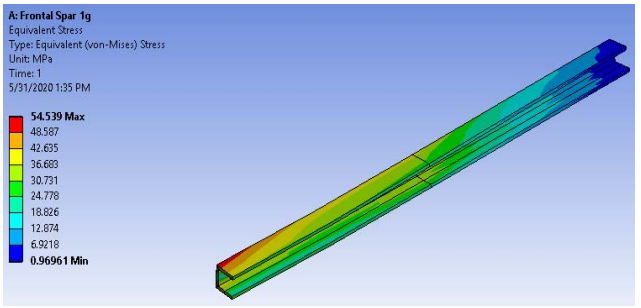

Fig. 20: Von Mises's Stress at 1g condition

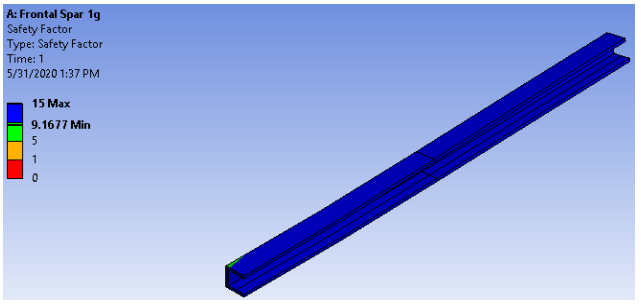

Fig. 21: Factor of Safety at 1g condition

Table 20: ANSYS Results for Front Spar using Steel

G's Values	Von Mises's Stress (MPa)	Factor of Safety
-1 g	36.96	13.53
-2 g	73.91	6.76
-3 g	110.83	4.51
-4 g	147.83	3.38
1 g	54.54	9.17
2 g	109.08	4.58
3 g	163.62	3.05
4 g	218.16	2.29
5 g	272.7	1.83
6 g	327.24	1.53

Table 21: ANSYS Results for Front Spar using Titanium

G's Values	Von Mises's Stress (MPa)	Factor of Safety
-1 g	40.03	42.47
-2 g	80.06	21.23
-3 g	120.08	14.16
-4 g	160.11	10.62
1 g	49.76	34.16
2 g	99.51	17.08
3 g	149.27	11.39
4 g	199.02	8.54
5 g	248.78	6.83
6 g	298.53	5.69
7 g	348.29	4.88

Error in FOS for Steel $= \frac{1.67-1.53}{1.67} \times 100 = 8.38\%$

Error in FOS for Titanium $= \frac{5.15-4.88}{5.15} \times 100 = 5.24\%$

Comparison of Results

Table 22: Comparison of Results

Aircraft Member	Analytical	Computational	% Error (Structural Steel)
Main Spar	1.29	1.66	22.3 %
Front Spar	1.25	1.53	18.3 %
Rear Spar	0.535	0.64	16.4 %

Aircraft Member	Analytical	Computational	% Error (Titanium)
Main Spar	2.99	2.25	24.7 %
Front Spar	5.15	4.88	5.2 %
Rear Spar	0.52	0.62	16 %

Discussion

The results obtained shows acceptable error percentage. The large error in results is due to reasons that certain approximations were made in analytical calculations i.e. concentrated load was used in cantilever beams while in ANSYS simulation uniformly distributed load was used.

5. Spar Models

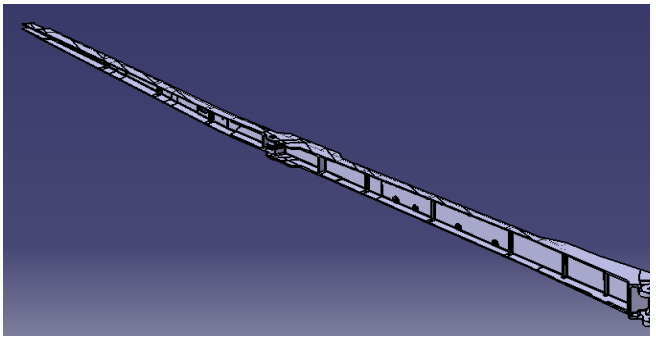

Fig. 22: Front Spar

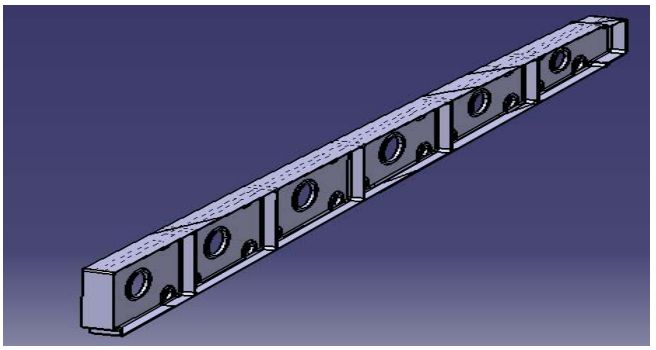

Fig. 23: Main Spar

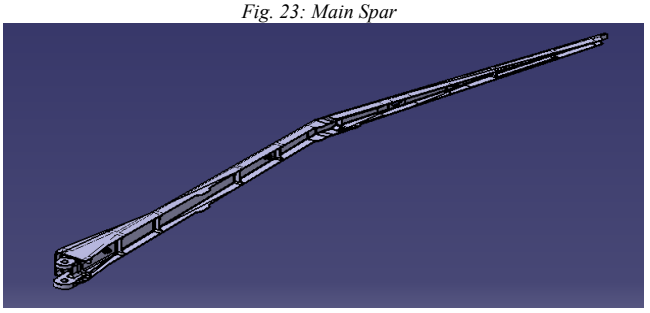

Fig. 24: Rear Spar

6. Materials

Materials Used in Spars are,

1) Structural Steel

2) Ti-6Al-2Zr-2Sn-2Mo-2Cr-0.25Si

3) Steel ph 13-8

7. Meshing

The meshing of spars is done using fine meshing technique and 1mm mesh size is used.

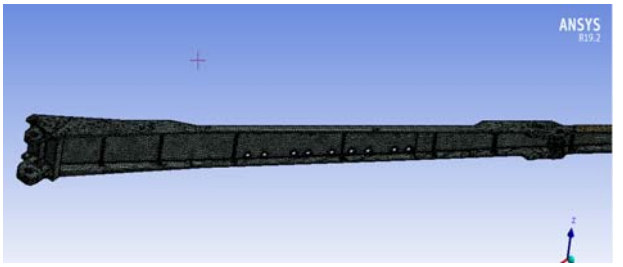

Fig. 25: Meshing of Front Spar

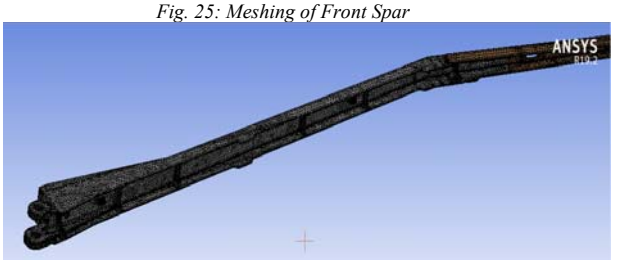

Fig. 26: Meshing of Rear Spar

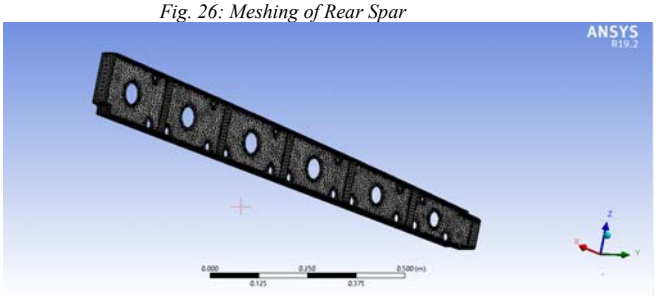

Fig. 27: Meshing of Main Spar

8. Boundary Conditions

Following boundary conditions are used in wing spars in ANSYS

- Spars are fixed from attachment points
- Uniform and elliptical pressure is applied to lower surface of wing in upward direction i.e. while pulling g's, lift force is increased and it is directed upward to support the aircraft in pulling those g's.
- Standard Gravitational acceleration is applied in downward direction.

Standard gravitational acceleration is applied downward so when an aircraft will pull certain amount of g's the lift force will increase which is required in pulling these g's conditions. For example, if an aircraft is pulling 4 g's the weight of aircraft on its wings will increase by 4 times from actual weight and so an increase in lift force will be required to support the aircraft. The wing tip is moving upward to help in providing necessary lift and pulling g's.

Uniform pressure:

Below are the boundary conditions for structural steel and titanium Ti-6Al-2Zr-2Sn-2Mo-2Cr-0.25Si for spars having uniform pressure distribution applied.

The spars are fixed from attachment points. Standard Earth gravity is applied for all loading conditions. Uniform pressure is applied on lower side of each spars.

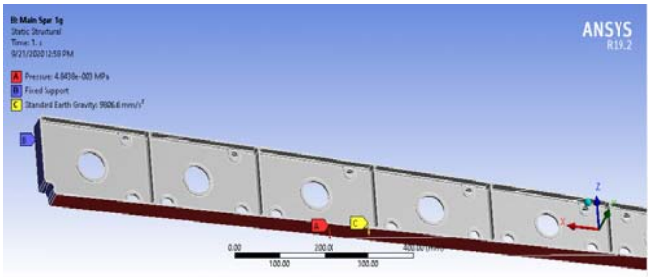

Fig. 38: Main Spar Boundary Conditions

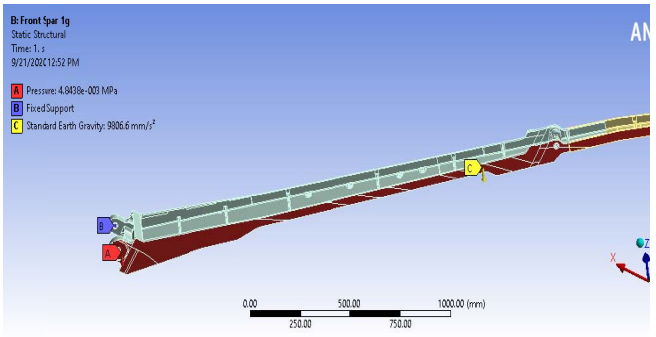

Fig. 39: Front Spar Boundary Conditions

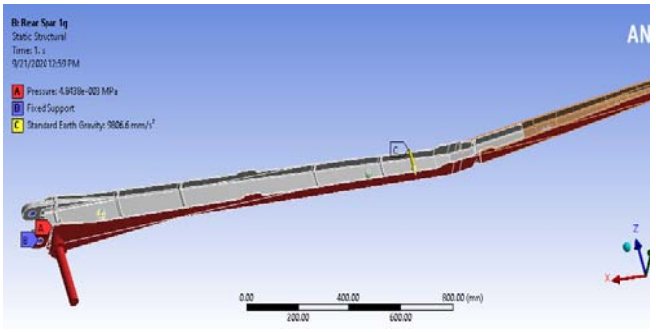

Fig. 40: Rear Spar Boundary Conditions

Elliptical Pressure:

Below are the boundary conditions for all spars having elliptical pressure distribution.

For elliptical loading, whole length of spar is divided in 15 equal parts and pressure is distributed elliptically and is applied on lower side of each spar. Standard Earth gravity is applied for all loading conditions.

All pressure values are calculated using below equation,

$$w = w_0\left[1 - \frac{x^2}{L^2}\right]$$

The distribution obtained for each load factor condition is displayed in tables in elliptical pressure distribution section of wing model.

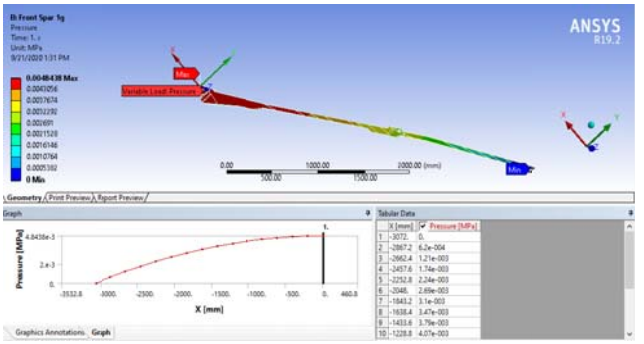

Fig. 41: Front Spar Boundary Conditions (Elliptical)

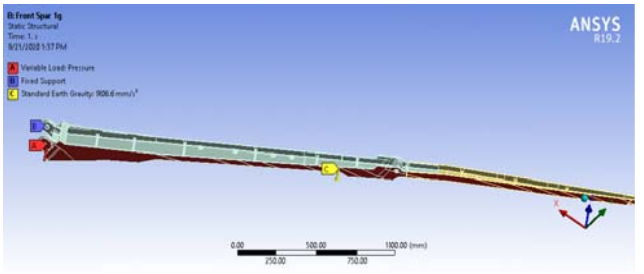

Fig. 42: Front Spar Boundary Conditions (Elliptical)

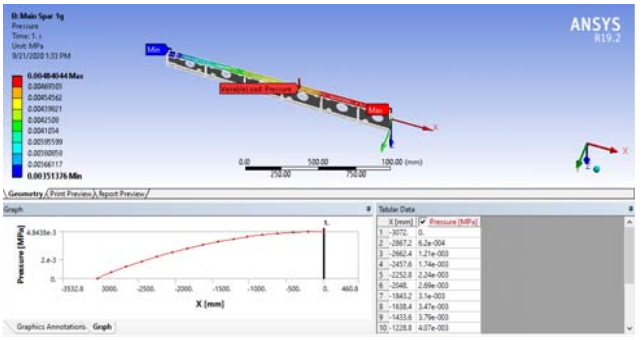

Fig. 43: Main Spar Boundary Conditions (Elliptical)

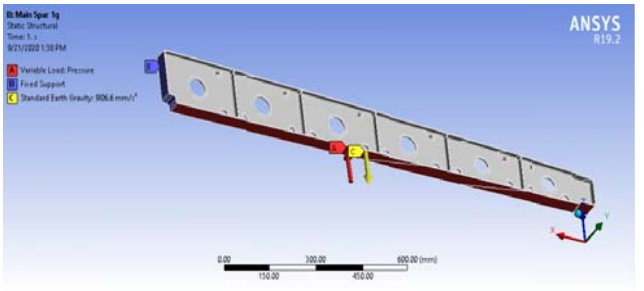

Fig. 44: Main Spar Boundary Conditions (Elliptical)

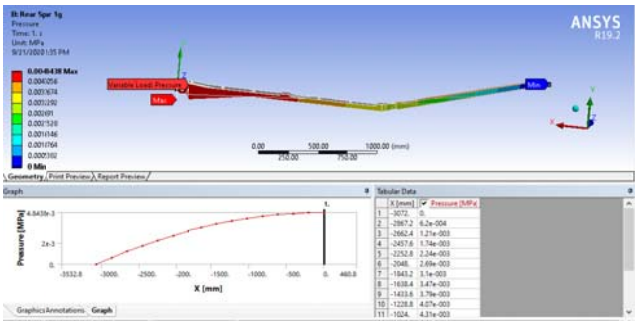

Fig. 45: Rear Spar Boundary Conditions (Elliptical)

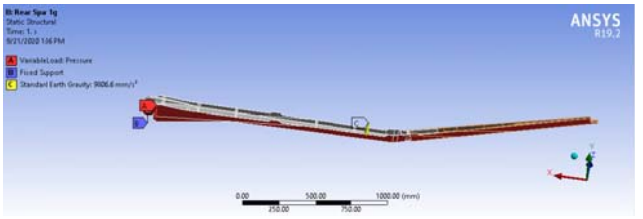

Fig. 46: Rear Spar Boundary Conditions (Elliptical)

10. Identification of Critical Stresses

The below figures show critical stress locations on spars using steel and titanium as material. Uniform and elliptical pressure is applied and their results are shown separately in below figures and tables.

- ***Uniform Pressure***

The results using structural steel (yield strength of 960 MPa) are shown in figures below

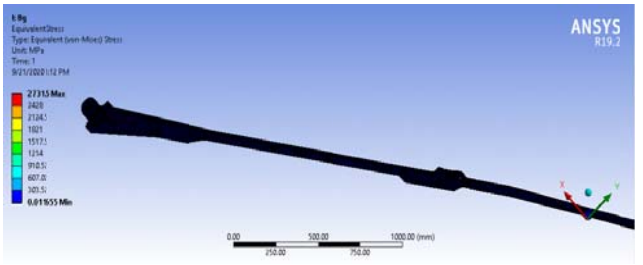

Fig. 47: Front Spar Critical Stress

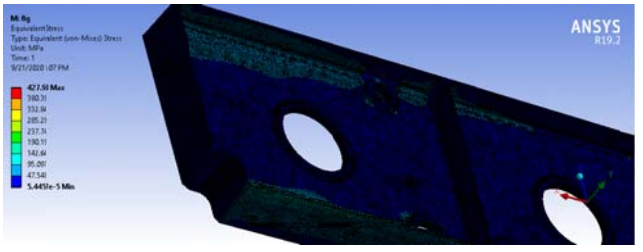

Fig. 48: Main Spar Critical Stress

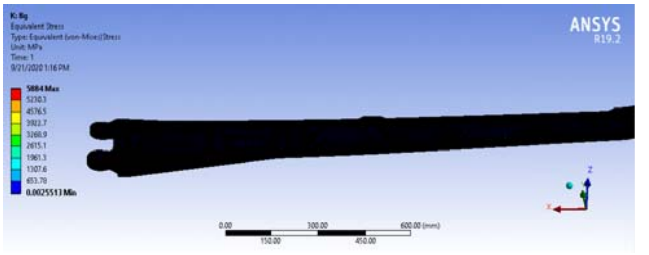

Fig. 49: Rear Spar Critical Stress

ANSYS Simulation Results

Table 23: ANSYS Results

g's Value	*Pressure (Pa)*	*Main Spar Von Misses (Mpa)*	*Front Spar Von Misses (Mpa)*	*Rear Spar Von Misses (Mpa)*
-1g	*4843.81*	*65.59*	*49.29*	*100.04*
-2g	*9687.62*	*118.2*	*88.5*	*183.79*
-3g	*14531.43*	*172.82*	*127.7*	*267.6*
1g	*4843.81*	*45.64*	*29.11*	*67.49*
2g	*9687.62*	*100.25*	*68.31*	*151.24*
3g	*14531.43*	*154.86*	*107.51*	*235*
4g	*19375.24*	*209.48*	*146.71*	*318.76*
5g	*24219.05*	*264.09*	*185.91*	*402.51*
6g	*29062.86*	*318.71*	*225.11*	*486.27*
7g	*33906.67*	*373.32*	*264.31*	*570.03*
8g	*38750.481*	*427.93*	*303.52*	*38750.48*

Discussion:

The above result shows that main spar and front spar can withstand all stresses without failing however, rear spar fails at 8g loading condition for structural steel.

All above results are simulated for stresses by comparing them with yield stress of materials used in construction of these spars i.e. structural steel and it has yield strength of 960 MPa.

The locations of critical stresses are at attachment point of spars with fuselage.

So, 7g is maximum allowed g pull condition for uniform loading if spars are made of structural steel.

The results using Titanium Ti-6Al-2Zr-2Sn-2Mo-2Cr-0.25Si (Yield Strength of 1010 MPa) are shown in figures below,

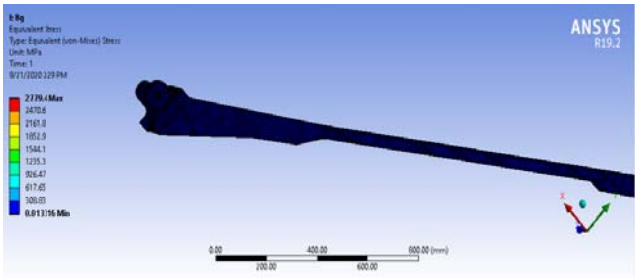

Fig. 50: Front Spar Critical Stress

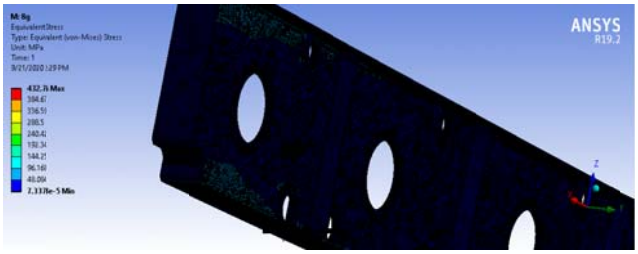

Fig. 51: Main Spar Critical Stress

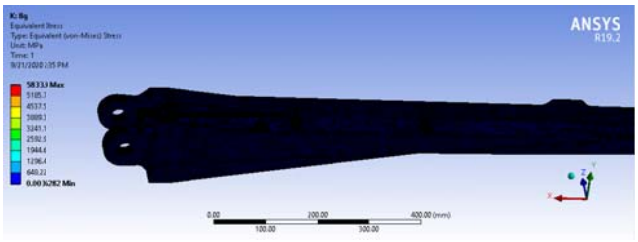

Fig. 52: Rear Spar Critical Stress

ANSYS Simulation Results

Table 24: ANSYS Results

g's Value	*Pressure (Pa)*	*Main Spar Von Misses (Mpa)*	*Front Spar Von Misses (Mpa)*	*Rear Spar Von Misses (Mpa)*
-1g	*4843.81*	*60.12*	*45.356*	*91.73*
-2g	*9687.62*	*114.88*	*84.71*	*173.95*
-3g	*14531.43*	*169.65*	*124.06*	*237.13*
1g	*4843.81*	*49.41*	*33.35*	*72.7*
2g	*9687.62*	*104.17*	*72.71*	*154.92*
3g	*14531.43*	*158.94*	*112.06*	*237.13*
4g	*19375.24*	*213.7*	*151.42*	*319.35*
5g	*24219.05*	*268.46*	*190.77*	*401.57*
6g	*29062.86*	*323.23*	*230.12*	*483.78*
7g	*33906.67*	*377.99*	*269.48*	*566*
8g	*38750.481*	*432.76*	*308.83*	*648.22*

Discussion:

The above result shows that all spars can withstand all stresses without failing if titanium Ti-6Al-2Zr-2Sn-2Mo-2Cr-0.25Si alloy is used as material.

These results are simulated for stresses against yield strength of titanium alloy.

- ***Elliptical Pressure***

The results using structural steel (yield strength of 960 MPa) are shown in figures below

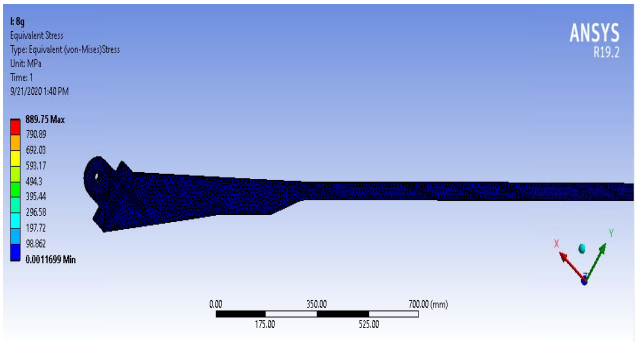

Fig. 53: Front Spar Critical Stress (Elliptical)

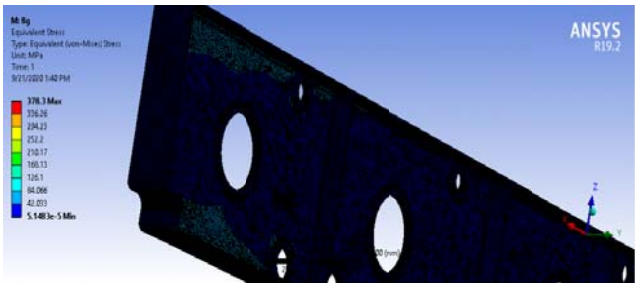

Fig. 54: Main Spar Critical Stress (Elliptical)

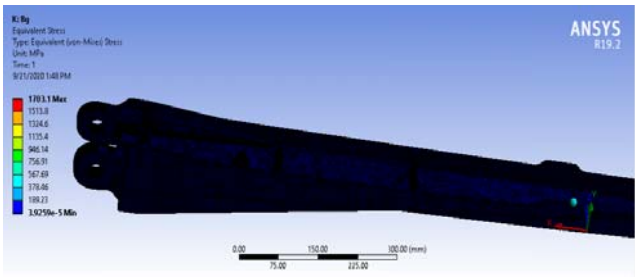

Fig. 55: Rear Spar Critical Stress (Elliptical)

ANSYS Simulation Results

Table 25: ANSYS Results

g's Value	*Pressure (Pa)*	*Main Spar Von Misses (Mpa)*	*Front Spar Von Misses (Mpa)*	*Rear Spar Von Misses (Mpa)*
-1g	*4843.81*	*58.42*	*61.43*	*71.25*
-2g	*9687.62*	*105.97*	*178.05*	*173.66*
-3g	*14531.43*	*152.27*	*300.76*	*278.52*
1g	*4843.81*	*37.88*	*39.52*	*37.79*
2g	*9687.62*	*84.71*	*155.57*	*140.45*
3g	*14531.43*	*131.57*	*279.19*	*244.68*
4g	*19375.24*	*178.4*	*400.11*	*346.04*
5g	*24219.05*	*225.21*	*522.43*	*448.74*
6g	*29062.86*	*272.05*	*644.83*	*551.51*
7g	*33906.67*	*315.96*	*766.85*	*653.42*
8g	*38750.481*	*378.3*	*889.75*	*756.91*

Discussion:

The above results show that main spar can withstand all loads however front spar fails at 6g and rear spar fails at 7g loading condition.

So, 5g is maximum allowed g pull condition for front spar and 6g is maximum allowed condition for rear spar.

The location of these critical stresses is at attachment points of spars with fuselage. So, when these spars fail it means that they will break or will form cracks if loaded beyond above mentioned maximum allowed loading conditions.

The results using Titanium Ti-6Al-2Zr-2Sn-2Mo-2Cr-0.25Si (Yield Strength of 1010 MPa) are shown in figures below,

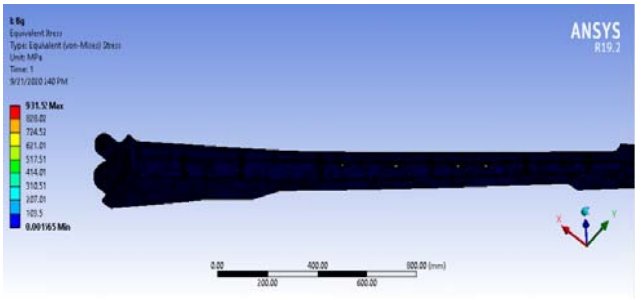

Fig. 56: Front Spar Critical Stress (Elliptical)

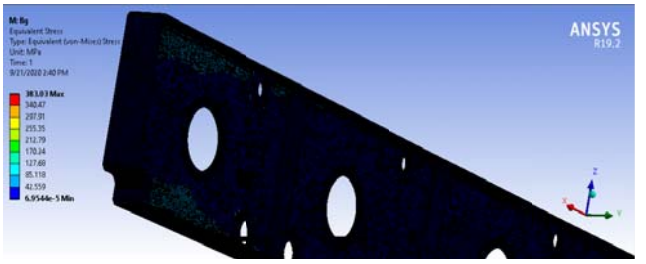

Fig. 57: Main Spar Critical Stress (Elliptical)

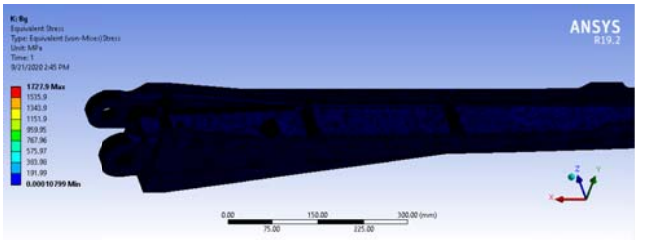

Fig. 58: Rear Spar Critical Stress (Elliptical)

ANSYS Simulation Results

Table 26: ANSYS Results

g's Value	*Pressure (Pa)*	*Main Spar Von Misses (Mpa)*	*Front Spar Von Misses (Mpa)*	*Rear Spar Von Misses (Mpa)*
-1g	*4843.81*	*52.77*	*67.38*	*82.97*
-2g	*9687.62*	*99.13*	*163.06*	*184.22*
-3g	*14531.43*	*145.79*	*258.18*	*286.45*
1g	*4843.81*	*41.63*	*54.49*	*62.64*
2g	*9687.62*	*88.59*	*150.06*	*163.49*
3g	*14531.43*	*135.58*	*246.89*	*265.7*
4g	*19375.24*	*182.54*	*341.51*	*365.09*
5g	*24219.05*	*229.49*	*437.21*	*465.79*
6g	*29062.86*	*276.46*	*532.95*	*566.56*
7g	*33906.67*	*320.49*	*628.39*	*666.48*
8g	*38750.481*	*383.03*	*724.52*	*767.96*

Discussion:

The above calculated results show that main spar carries all loads without failing however front spar and rear spar fails at 8g loading conditions.

So, 7g is maximum allowed g pull condition for both front and rear spar and if loaded beyond this i.e. if aircraft will pull beyond 7g, front and rear spar will fail.

The location of these critical stresses is at attachment point of spars.

11. *Meshing of Wing Model*

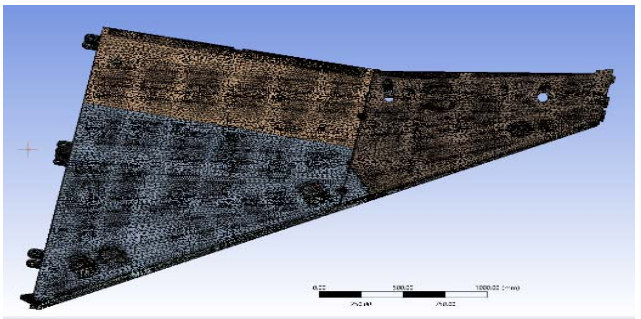

Fig. 59: Meshing of wing model in ANSYS

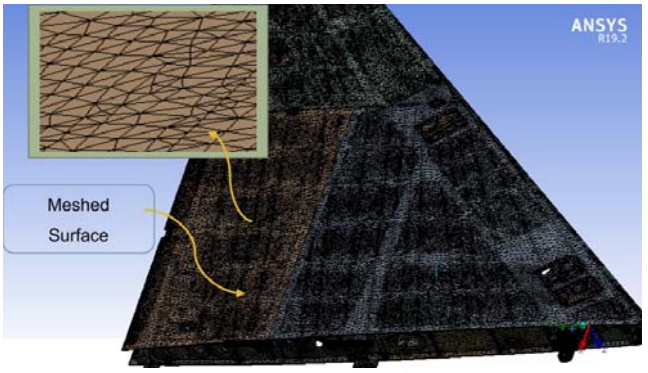

Fig.60: Meshed Surface of wing

Table 27: Meshing Sizes

Wing Part	Mesh Element Size
Spars	5 mm
Remaining all Parts	10 mm

Fig.61: Internal Structural MemberMeshing

12. *Boundary Conditions*

Wing is fixed from holes at attachment points of spars with fuselage and uniform pressure and uniformly varying pressure is applied to lower surface of wing.

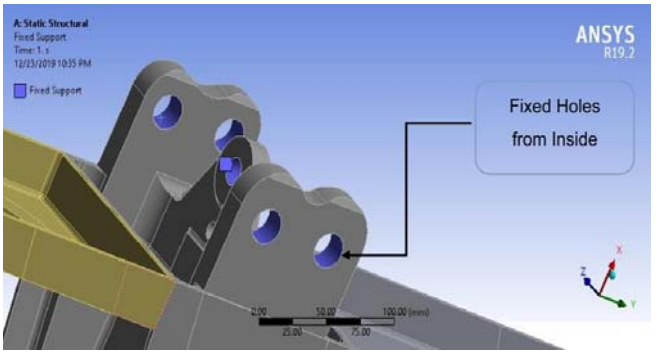

Fig. 62: Fixed End holes of Main Spar

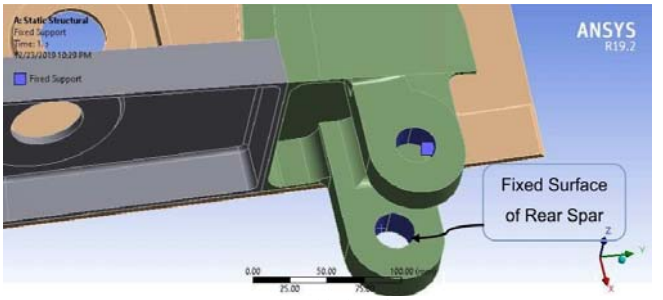

Fig. 63: Fixed End holes of Rear Spar

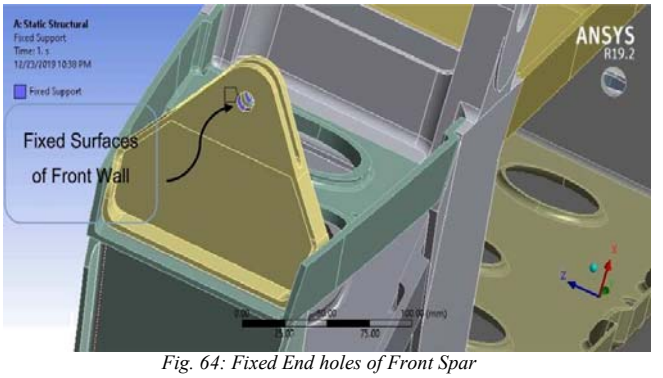

Fig. 64: Fixed End holes of Front Spar

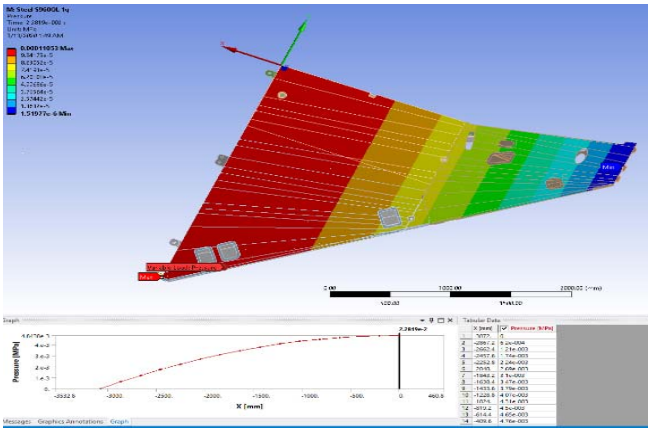

Fig. 65: Elliptically Distributed Pressure on lower surface of wing

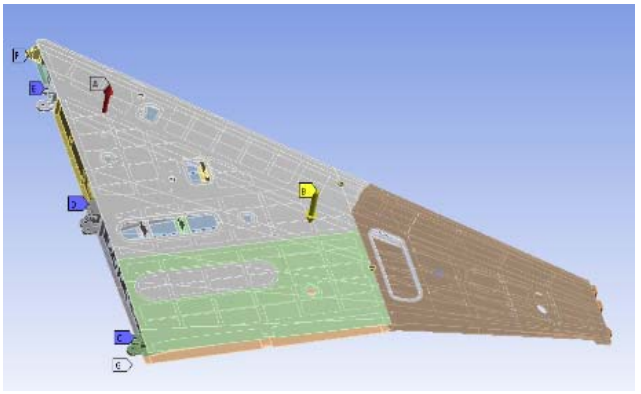

Fig. 66: Applied Boundary Conditions i.e. Uniform pressure applied upward and gravitational acceleration applied downward

Apartfromtheuniformpressureloadingappliedtothemodel.Acceleration load will be applied to the whole wing which will be equal to the corresponding load factor. In ANSYS we applied the acceleration load is applied to the all parts of geometry as per there weight. The acceleration will be applied in downward direction in case of positive load factor and will be applied upward in case of negative load factor. For +1 gitsvaluewillbe9.81m/sec^{2}andfor+2gitsvaluebe19.62m/sec^{2}and dwillbeapplied downward and for value of +8 G's it can be seen in figure andtable.

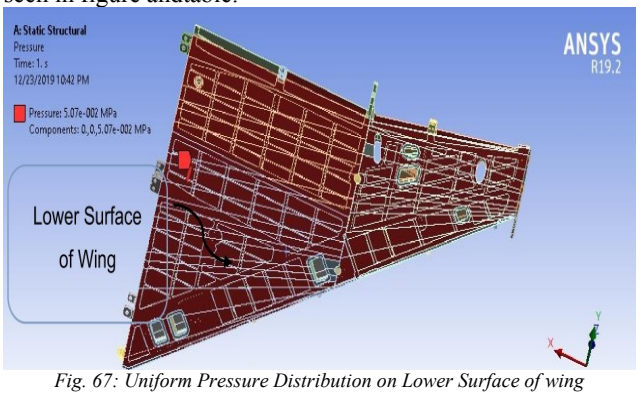

Fig. 67: Uniform Pressure Distribution on Lower Surface of wing

13. Identification of Critical Stresses

The below fig. shows stresses obtained using uniform pressure distribution

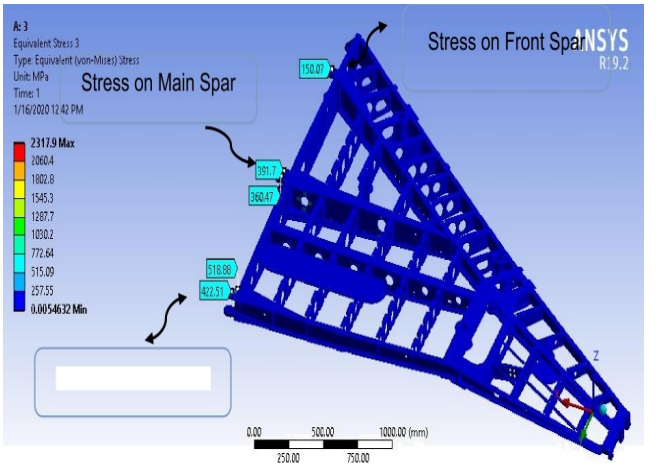

Fig. 68: Identification of critical stress

- **Elliptical Pressure Distribution:**

The elliptical pressure distribution on wing will be calculated using following equation,

$$w = w_0[1 - \frac{x^2}{L^2}]$$

In above equation,

L = 3072 mm (Total length of wing)

w_0= Pressure values for different load factors

If we divide whole wing in 15 equal parts then,

Table 28: x values

x
204.8
409.6
614.4
819.2
1024
1228.8
1433.6
1638.4
1843.2
2048
2252.8
2457.6
2662.4
2867.2

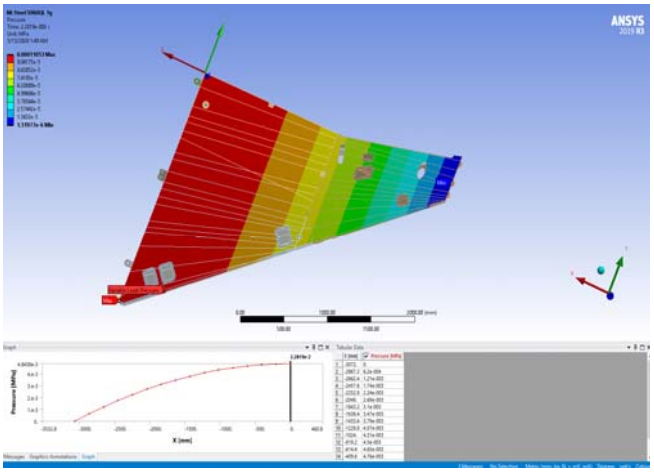

Fig. 69: Elliptically Distributed Pressure on wing

The above fig. shows elliptical pressure distribution on wing using tabular data.

The below table shows results of critical stresses using elliptical pressure distribution.

Table 29: Results using elliptical pressure distribution

G's Values	Main Spar Von Mises (MPa)	Rear Spar Von Mises (MPa)	Front Spar Von Mises (MPa)
-1g	*97.542*	*328.61*	*887.43*
-2g	*195.08*	*657.21*	*1774.9*
-3g	*292.62*	*985.78*	*2662.2*
1g	*123.78*	*427.07*	*1159.2*
2g	*247.57*	*854.14*	*2318.5*
3g	*371.34*	*1281.2*	*3477.6*
4g	*495.13*	*1708.3*	*4636.9*
5g	*618.92*	*2135.4*	*5796.2*
6g	*742.71*	*2562.4*	*6955.5*
7g	*866.5*	*2989.5*	*8114.8*

Discussion

The tables show results for Von Mises stress at each spar under different loading conditions. Elliptically distributed loads are applied on spars to obtain critical stresses.

The results calculated shows that main spar can withstand all loads without failing while front spar fails at 4g and rear spar fails at -2g and 2g loading conditions.

The location of these critical stresses is at attachment point of spars with fuselage.

III. DISCUSSION ON RESULTS

The results for analysis of wing spars and wing model is obtained separately. For both analysis uniform and elliptical pressure distribution is used for simulation in ANSYS. The discussion on results obtained from each analysis is done below.

A. Discussion on results obtained from analysis on wing spars in ANSYS:

The results for Von Mises stress at each spar under different loading conditions are obtained for identification of critical stresses on each spar. Two different materials are used i.e. structural steel and titanium Ti-6Al-2Zr-2Sn-2Mo-2Cr-0.25Si. Uniformly distributed and elliptically distributed pressure is applied on spars to obtain critical stresses. The results for both pressure distribution for both materials are discussed below.

- **Uniform Pressure**

The result shows that main spar and front spar can withstand all stresses without failing however, rear spar fails at 8g loading condition for structural steel. All results are simulated for stresses by comparing them with yield stress of materials used in construction of these spars i.e. structural steel and it has yield strength of 960 MPa. The locations of critical stresses are at attachment point of spars with fuselage. So, 7g is maximum allowed g pull condition for uniform loading if spars are made of structural steel.

The result shows that all spars can withstand all stresses without failing if titanium Ti-6Al-2Zr-2Sn-2Mo-2Cr-0.25Si alloy is used as material. These results are simulated for stresses against yield strength of titanium alloy.

- **Elliptical Pressure**

The results for structural steel show that main spar can withstand all loads however front spar fails at 6g and rear spar fails at 7g loading condition. So, 5g is maximum allowed g pull condition for front spar and 6g is maximum allowed condition for rear spar. The location of these critical stresses is at attachment points of spars with fuselage. So, when these spars fail it means that they will break or will form cracks if loaded beyond above mentioned maximum allowed loading conditions.

The calculated results for titanium Ti-6Al-2Zr-2Sn-2Mo-2Cr-0.25Si show that main spar carries all loads without failing however front spar and rear spar fails at 8g loading conditions. So, 7g is maximum allowed g pull condition for both front and rear spar and if loaded beyond this i.e. if aircraft will pull beyond 7g, front and rear spar will fail. The location of these critical stresses is at attachment point of spars.

B. Discussion on results obtained from analysis on wing model in ANSYS:

For wing model, uniform and elliptical pressure distribution is applied to obtain respective results of critical stresses separately for both. The material used for each part of wing model for analysis in both cases are listed in material properties section. However, for spars steel and titanium Ti-6Al-4V is used as materials.The tables show results for Von Mises stress at each spar underdifferent loading conditions. For uniform pressure, all spars withstand applied load without failing however for elliptically distributed loads applied on spars to obtain critical stresses, the results simulated shows that main spar can withstand all loads without failing while front spar fails at 4g and rear spar fails at -2g and 2g loading conditions.The location of these critical stresses is at attachment point of spars with fuselage.

IV. CONCLUSION

Static structural analysis of wing spars that are made of steel and titanium was carried out to determine the location and value of critical stress locations at different g's values and find out minimum factor of safety of spars.

For estimation of critical stress locations and factor of safety of spar,

- First, pressure value was calculated that will act as load value on spars.
- Since spars are fixed from one end i.e. attachment point with fuselage so they will be acting like cantilever beams.

Analytical calculation:

- Analytical calculation was done using uniform pressure distribution on cantilever beam
- Then CATIA Models of I and C beams having same dimensions for beams as used for analytical calculation were made and simulation was done in ANSYS for critical stresses using uniform pressure distribution.
- Values of bending stress and shear stress were calculated and then Von Mises's stress is calculated for each spar beam.

Material:

- Structural Steel and Titanium Ti-6Al-2Zr-2Sn-2Mo-2Cr-0.25Si were used as materials and their material properties were added in engineering data in ANSYS workbench and using their respective yielding strengths, value of equivalent stress and minimum factor of safety was calculated.

ANSYS Simulation:

- The CATIA models of spar beams were imported in ANSYS workbench for structural analysis and values of Von Mises's stress and factor of safety is calculated.
- The pressure was distributed uniformly over spar beams.
- The values calculated analytically and using ANSYS were compared.
- The results show that Spars of wings can withstand 8g's load without failing and critical stress locations were found near attachment points of spars with fuselage.
- Then individual CAD model of spars were imported in ANSYS and then uniform and elliptical pressure was applied to simulate critical stresses.
- The results for both materials with uniform and elliptical pressure were discussed separately in discussion chapter.
- The CAD model of wing was imported in ANSYS and static structural analysis was carried out using uniform and elliptical pressure distribution and the results show that critical stress locations were near attachment points of spars with fuselage.

Discussion on results:

- The solutions obtained using steel as material gives acceptable results but using titanium gives better results. The main reason is that titanium has better strength to weight ratio and it also resists cavitation and erosion that makes it to appropriate to use in high stress applications.
- The error in analytical calculation and ANSYS simulation results is very small and difference in values of Factor of Safety is also very small in both the cases.

V. LIMITATIONS

Certain assumptions were taken into account in the course of this research which were mentioned in each section. These assumptions pose some limitation on this work. These limitations are outline here.
Assumptions taken during the Finite Element Analysis are presentedbelow,

- Weightassumedtobeconstantthroughouttheflight.Aconstantweight assumption will produce severe loadingcondition
- The assumption that is taken that 95% lift isproduced by the wings of the aircraftonly
- A constant pressure distribution was assumed on the complete wing of the aircraft which corresponds to severloads.

VI. RECOMMENDATIONS

The recommendations and future work for research are

- Fatigue Life estimation can be carried out using results obtained in this research for spars.
- Actual Load Spectrum can be used to determine accumulative damage using Miner's rule.
- This technique can be applied to any aircraft.

- Variation in weight must be considered since uniform weight is considered throughout the analytical calculations.
- Analytical Calculation is carried out in cruise condition but different conditions can be used in calculation of load or pressure value.
- Different materials can be tested using this technique for construction of Spars.

VII. REFERENCES

[1] Garre, Parthasarathy, and G. Venkata Arjun. "Modeling and analysis of a RIBS and Spars of an airplane wing for bending and shear loads." *International Journal for Research in Applied Science and Engineering* 5.2 (2017): 295-315.

[2] Shabeer, K. P., and M. A. Murtaza. "Optimization of aircraft wing with composite material." *International Journal of Innovative Research in Science, Engineering and Technology* 2.6 (2013).

[3] Tamura, Satoru, and SF BUSSAMRA. "A Simplified Geometric Method for Wing Loads Estimation." *3rd CTA-DLR Workshop on Data Analysis & Flight Control. SJ Campos*. 2009.

[4] Schrenk, Oskar. "A simple approximation method for obtaining the spanwise lift distribution." (1940).

[5] Soemaryanto, Arifin Rasyadi, and Nurhayyan Halim Rosid. "Verification of Schrenk Method for Wing Loading Analysis of Small Unmanned Aircraft Using Navierstokes Based CFD Simulation." *JurnalTeknologiDirgantara* 15.2 (2018): 161-166.

[6] Hinton, M. J. K. A., P. D. Soden, and Abdul-Salam Kaddour, eds. *Failure criteria in fibre reinforced polymer composites: the world-wide failure exercise*. Elsevier, 2004.

[7] Mangurian, George N. *The aircraft structural factor of safety*. No. AGARD-154. ADVISORY GROUP FOR AERONAUTICAL RESEARCH AND DEVELOPMENT PARIS (FRANCE), 1957.

[8] Modlin, C. T., and J. J. Zipay. "The 1.5 & 1.4 Ultimate Factors of Safety for Aircraft & Spacecraft-History, Definition and Applications." (2014).Megson, T. H. G. "Aircraft structures for engineering students [electronic resource]." (2013).

[9] Deng, S., and Tsung-Han Yeh. "Applying least squares support vector machines to the airframe wing-box structural design cost estimation." *Expert Systems with Applications* 37.12 (2010): 8417-8423.

[10] Sobieszczanski-Sobieski, Jaroslaw, and Raphael T. Haftka. "Multidisciplinary aerospace design optimization: survey of recent developments." *Structural optimization* 14.1 (1997): 1-23.

[11] Petrašinović, Danilo, BoškoRašuo, and Nikola Petrašinović. "Extended finite element method (XFEM) applied to aircraft duralumin spar fatigue life estimation." *Tehničkivjesnik* 19.3 (2012): 557-562.

[12] Gruszecki, J., and A. Tomczyk. "Landing augmentation system for general aviation aircraft: analysis and simulation." *Systems Science* 25.4 (1999): 63-70.

[13] Raymer, Daniel. *Aircraft design: a conceptual approach*. American Institute of Aeronautics and Astronautics, Inc., 2012.

[14] Michael Bauccio (1993), ASM Metals Reference Book, 3rdEdition, ASM International, Materials Park, OH

[15] Baker, A., ed. *Bonded repair of aircraft structures*. Vol. 7. Springer Science & Business Media, 2012.

[16] Atmeh, Ghassan M., Zeaid Hasan, and Feras Darwish. "Design and stress analysis of a general aviation aircraft wing." *Excerpt from the Proceedings of the COMSOL Conference 2010 Boston*. 2010.

[17] Peruru, Sivarama Prasad, and Suman Babu Abbisetti. "Design and finite element analysis of aircraft wing using ribs and spars." *Int. Res. J. Eng. Technol.(IRJET)* 4.i. 06 (2017): 2133-2139.

[18] Kumar, TJ Prasanna, et al. "DESIGN AND STRESS ANALYSIS OF SWEPT BACK WING WITH NASTRAN AND PATRAN." (2018).

[19] ELANGOVAN, S., C. SURESHKUMAR, and P. DIVYABARATHI. "DESIGN AND ANALYSIS OF AIRCRAFT WING SPAR WITH DIFFERENT MATERIALS USING ANSYS."

[20] Girennavar, Mutturaj, et al. "Design, Analysis and Testing of Wing Spar for Optimum Weight." *International Journal of Research and Scientific Innovation (IJRSI)* 4.VII (2017): 104-112.

[21] Kovalovs, Andrejs, EvgenyBarkanov, and SergejsGluhihs. "Active twist of model rotor blades with D□spar design." *Transport* 22.1 (2007): 38-44.

[22] Abid-Aun, Salah H., Shawkat J. AL-Tornachi, and Muhsin J. Jweeg. "Optimization of light weight aircraft wing structure." *Journal of Engineering and Sustainable Development* 12.1 (2008): 1-22.

[23] Kaufmann, Markus, Thomas Czumanski, and Dan Zenkert. "Manufacturing process adaptation for integrated cost/weight optimisation of aircraft structures." *Plastics, rubber and composites* 38.2-4 (2009): 162-166.

[24] Torenbeek, Egbert. *Advanced aircraft design: conceptual design, analysis and optimization of subsonic civil airplanes*. John Wiley & Sons, 2013.

[25] Kennedy, Graeme, and Joaquim Martins. "A comparison of metallic and composite aircraft wings using aerostructural design optimization." *12th AIAA Aviation Technology, Integration, and Operations (ATIO) Conference and 14th AIAA/ISSMO Multidisciplinary Analysis and Optimization Conference*. 2012.

[26] Findlay, S. J., and N. D. Harrison. "Why aircraft

fail." *Materials today* 5.11 (2002): 18-25.
[27] Collins, Jack A. *Failure of materials in mechanical design: analysis, prediction, prevention*. John Wiley & Sons, 1993.
[28] Girennavar, Mutturaj, et al. "Design, Analysis and Testing of Wing Spar for Optimum Weight." *International Journal of Research and Scientific Innovation (IJRSI)* 4.VII (2017): 104-112.
[29] Dutt, K. Mahesh. "Damage Tolerance Evaluation of the Front Spar in a transport aircraft wing."
[30] Shah, Surendra P., Stuart E. Swartz, and Chengsheng Ouyang. *Fracture mechanics of concrete: applications of fracture mechanics to concrete, rock and other quasi-brittle materials*. John Wiley & Sons, 1995.
[31] "Major Components of an Aircraft*." Rod Machado's Private Pilot Handbook, www.flightliteracy.com/major-components-of-an-aircraft.htm*
[32] Chintapalli, Sridhar, et al. "The development of a preliminary structural design optimization method of an aircraft wing-box skin-stringer panels." *Aerospace Science and Technology* 14.3 (2010): 188-198.
[33] Schuhmacher, Gerd, et al. "Multidisciplinary design optimization of a regional aircraft wing box." *9th AIAA/ISSMO Symposium on Multidisciplinary Analysis and Optimization*. 2002.
[34] Sues, Robert, Mohammad Aminpour, and Youngwon Shin. "Reliability based MDO for aerospace systems." *19th AIAA Applied Aerodynamics Conference*. 2000.
[35] "Wings of the future." Airbus, 17 Jan. 2017, www.airbus.com/newsroom/news/en/2017/01/Wings-of-the-future
[36] Taylor, Robert M., and Terrence A. Weisshaar. *Improved structural design using evolutionary finite element modeling*. PURDUE UNIV LAFAYETTE IN SCHOOL OF AERONAUTICS AND ASTRONAUTICS, 2003.
[37] Tiwari, Ashutosh, et al. "Automated inspection using database technology within the aerospace industry." *Proceedings of the Institution of Mechanical Engineers, Part B: Journal of Engineering Manufacture* 222.2 (2008): 175-183.
[38] Hürlimann, F., et al. "Investigation of local load introduction methods in aircraft pre-design." *Aerospace Science and Technology* 21.1 (2012): 31-40.
[39] Zhu, Ji-Hong, Wei-Hong Zhang, and Liang Xia. "Topology optimization in aircraft and aerospace structures design." *Archives of Computational Methods in Engineering* 23.4 (2016): 595-622.
[40] Megson, Thomas Henry Gordon. *Aircraft structures for engineering students*. Butterworth-Heinemann, 2016.
[41] Maruyama, Ippei, et al. "Flexural properties of reinforced recycled concrete beams." *Proceedings of the international RILEM conference on the use of recycled materials in buildings and structures, Barcelona, Spain*. 2004.
[42] Stefanovic, Milan, et al. "Simulation driven weight optimization of a composite UAV spar using multiscale analysis." (2010).
[43] Schrenk, Oskar. "A simple approximation method for obtaining the spanwise lift distribution." (1940).
[44] Metals Handbook, Vol. 2 – "Properties and Selection: Nonferrous Alloys and Special Purpose Materials", ASM International 10th Edition 1990.
[45] "30CrMnSiA/30CrMnSiA Alloys Steel Plate." Mill Technical Information, China, gangsteel.net/product/alloy/GB/T3077/30CrMnSiA.html
[46] Chen, Chang, et al. "Simulation Analysis and Experimental Study on Strength Optimization of a Plug-In Oil Hose Joint." *Advances in Materials Science and Engineering* 2018 (2018).
[47] Bauccio Michael, "ASM Metals Reference book" Third Edition, Ed. ASM International, Materials Park, OH, 1993.
[48] R. Boyer, G. Welsch, E. Collings, eds. "Materials Properties Handbook: Titanium Alloys" ASM International, Material Park, OH, 1994.
[49] "Grade Ti-6Al-2Zr-2Sn-2Mo-2Cr-0.25Si Alloy", AZO Material, 9 Aug. 2013 www.azom.com/article.aspx?ArticleID=9367
[50] Wang, M., X. Lin, and W. Huang. "Laser additive manufacture of titanium alloys." *Materials Technology* 31.2 (2016): 90-97.
[51] Peters, Manfred, et al. "Titanium alloys for aerospace applications." *Advanced engineering materials* 5.6 (2003): 419-427.
[52] Crawford Bill, "Flight lab Ground School Maneuvering loads, High-G Maneuvers", Flight Emergency & Advanced Maneuvers Training, Inc. dba Flight lab, 2009